2014-03-01

West Antarctic Surface Mass Balance: Do Synoptic Scale Modes of Climate Contribute to Observed Variability?

McLean Kent Carpenter
Brigham Young University - Provo

West Antarctic Surface Mass Balance: Do Synoptic Scale Modes of Climate Contribute to Observed Variability?

McLean K. Carpenter

A thesis submitted to the faculty of
Brigham Young University
in partial fulfillment of the requirements for the degree of

Master of Science

Summer Rupper, Chair
Steve Nelson
Barry Bickmore
Gregory Carling

Department of Geological Sciences

Brigham Young University

March 2014

ABSTRACT

West Antarctic Surface Mass Balance: Do Synoptic Scale Modes of Climate Contribute to Observed Variability?

McLean K. Carpenter
Department of Geological Sciences, BYU
Master of Science

Western Antarctica has been experiencing significant warming for at least the past fifty years. While higher Net Surface Mass Balance (SMB) over West Antarctica during this period of warming is expected, SMB reconstructions from ice cores reveal a more complex pattern during the period of warming. The mechanisms giving rise to SMB variability over the West Antarctic Ice Sheet (WAIS) are not well understood due to lack of instrumental data. The Southern Annular Mode (SAM) and El Niño Southern Oscillation (ENSO) are believed to contribute to WAIS SMB variability but the assumption has not been rigorously tested. SMB during years where SAM and ENSO are in extreme phases is compared to average SMB from the period 1979-2010. Additionally, atmospheric circulation anomalies are used to assess what circulation patterns accompany extreme modes of climate during the same period.

The results suggest that significantly lower SMB occurs when SAM is in an extremely positive phase or ENSO is in an extremely negative phase. Additionally, atmospheric circulation anomalies show that certain circulation patterns accompany extreme modes of climate, which contribute to SMB variability over the WAIS. Ultimately, the location of low and high pressure cells is the best predictor for extreme accumulation events over the WAIS. These results are verified by assessing observed net SMB trends from a network of firn cores located from the central WAIS. Seven new firn cores are added to improve the spatial network of regional net SMB measurements. Reconstructed net SMB is calculated from new firn core records, and compared to the existing cores. The new suite of preliminary firn core records show the same significant decreasing trend that is observed in existing cores. This represents a negative region-wide SMB trend that is likely in part due to trends in SAM and ENSO.

Keywords: Climate Variability, West Antarctica, Surface Mass Balance, Ice Core

ACKNOWLEDGEMENTS

I would like to thank my advisor, Dr. Summer Rupper for the opportunity to be a part of her research group, and give me the opportunity to take on such an exciting and challenging project. I am very appreciative for the guidance and mentorship she provided for me over the past two years. I would like to thank my committee members, Drs. Steve Nelson, Barry Bickmore, and Greg Carling for their guidance and input during the length of this project.

I would like to thank Landon Burgener and Jessica Williams, as they provided me with the training and guidance needed for me to begin my project and take it to completion. I would like to thank the students in the climate dynamics lab who assisted me in the preliminary lab work which included processing the firn cores, entering data, and preparing samples for isotopic analysis. I would like to thank my wonderful wife Whitney for all of her support she has provided me throughout my schooling and the sacrifices she has made for me. I would like to thank my mom and dad for always setting an example of hard work for me and giving me the necessary tools to succeed in life.

Lastly and most importantly I would like to acknowledge the funding that made my thesis work possible. The support for this research work was provided by the National Science Foundation Office of Polar Programs Grant #094470 to SBR and #0944653 to RF

TABLE OF CONTENTS

LIST OF TABLES

LIST OF FIGURES

Part 1: Testing synoptic scale modes of climate

1. Introduction

[1] Changes in the mass balance of the polar ice sheets have global implications by changing global albedo, global sea level, and thermohaline ocean circulation. The West Antarctic Ice Sheet (WAIS), the region west of the Transantarctic Mountains, is a region that has experienced many changes in climate over the past 50 years (Thomas et al., 2008). For example, the WAIS has experienced significant warming over at least the past fifty years (Steig et al. 2009). In addition, the WAIS alone has the sea-rise potential of approximately 5 meters (Vaughan and Spouge, 2002). Recent net precipitation, sublimation, snow drift, and melt (Surface Mass Balance, SMB) in the Western Antarctica (WA) interior is poorly understood due to limited availability of instrumental data, coupled with the remoteness of the region (Naik, 2010). The variability in mass balance in response to climate variability is therefore of significant concern.

[2] The majority of global climate models simulate increases in SMB in response to warmer temperatures, largely due to the Clausius-Clapeyron effect. However, SMB reconstructions from ice cores reveal a more complex pattern in SMB over the period of warming. For example, SMB reconstruction from the Gomez core located on the southwestern Antarctic Peninsula (AP) show a significant increase in accumulation and 100-year warming trend (Thomas et al., 2009). A suite of firn cores near the Pine Island Glacier show no change in accumulation, while there is a statistically significant decline in accumulation over portions of the WAIS interior (Burgener et al., 2013, Medley et al.,2013). This non-uniform pattern may be in part due to changes in atmospheric circulation that are giving rise to the observed changes in temperature over the WAIS. Therefore, one significant question of interest is how the variability

of Southern Hemisphere (SH) atmospheric circulation affects West Antarctic SMB. WA is a region known to be affected by strong inter-annual variability that is thought to be at least partially related to climate variability in the lower latitudes (Kidson, 1999). Synoptic scale modes of climate are believed to be contributing to the SMB variability, although this assumption has not been rigorously tested. To better understand the variability of the WAIS SMB, it is necessary to assess whether synoptic scale modes of climate are contributing to the observed SMB variability.

2. Objectives

[3] The main objective of this research is to assess the influence of synoptic scale modes of climate on surface mass balance (SMB) in Western Antarctica. This will be accomplished by assessing how SMB varies when synoptic scale modes of climate are in extreme phases and by assessing the circulation patterns that accompany these extreme phases.

3. Background

[4] Western Antarctica has been warming significantly at a rate of 0.17 ± 0.06 degrees C per decade from 1957 to 2006, with the warming being strongest in the winter and spring months (Steig et al, 2009). The saturation vapor pressure of air increases rapidly and non-linearly with increasing temperatures, so warmer temperatures are expected to correspond to increased precipitation. However, recent SMB trends in central WAIS are negative in spite of the observed surface warming over the same region (Burgener et al., 2013). This SMB trend is also apparent in seven preliminary reconstructed records from the 2011 season (this study). Thus there is strong evidence for a region wide decrease in SMB, at least over the central WAIS region. One possible cause of a region wide decrease in SMB could be due to shifts in atmospheric

circulation in response to synoptic scale modes of climate. The question that arises is how do modes of climate affect SMB in central WAIS?

[5] The variability of southern hemisphere atmospheric circulation is dominated by the Southern Annular Mode (SAM), which was previously referred to as the "high latitude mode" and the "Antarctic Oscillation" (Thompson and Wallace 2000). The SAM is the principal mode of variability in the atmospheric circulation in the mid and high latitudes of the Southern Hemisphere (Naik et al, 2010). It represents the strengthening and weakening of the circumpolar vortex, which is the belt of tropospheric westerlies that surround the Antarctic continent, and provides a means of linking the Antarctic climate with that of lower latitudes via an atmospheric wave train (Turner, 2004). Variations in the SAM are caused by the seasonal shift in the subtropical upper level jet and in the intensity changes of the Southern Hemisphere polar jet (Carvalho, 2004). The storm track in the southern hemisphere exhibits substantial north-south migration associated with variations in the SAM (Ding and Steig, 2012).

[6] During the positive phase of SAM, extra tropical cyclones tend to stay more pole ward and have lower central pressures (stronger storms). During the negative phase of SAM, extra tropical cyclones form and move to lower latitudes and tend to have higher pressures in the center (weaker storms). The positive phase of SAM is characterized by an area of persistent low pressure off the west coast of Antarctica in the Amundsen Sea region (Ding and Steig 2012). Two prevailing mechanisms have been proposed to explain variability in the SAM. Long-term variability in the SAM has been attributed to the direct impact of radiative forcing (Pezza et al., 2012, Thompson and Solomon, 2002, Ding and Steig, 2012). The El Niño Southern Oscillation (ENSO) has also been dynamically linked to SAM, thus sea surface temperature changes in the tropics are thought to influence circulation patterns in the mid to high latitudes.

[7] The El Niño Southern Oscillation (ENSO) is the dominant mode of climate variability centered in the tropical pacific, and has an influence on weather patterns globally. The location of warm sea surface temperature pockets in the tropical Pacific shift depending on the phase of ENSO and cause temporary major shifts in global weather patterns. An important link between tropical sea surface temperatures (SST) anomalies and circulation variability in the high latitudes of the Southern Hemisphere has been recognized for decades (Ding and Steig, 2013). Multiple studies (Kwok and Comiso, 2002; Fogt and Bromwich 2006; Fogt et al. 2011) have shown that ENSO influences SAM, where the magnitude of the ENSO teleconnection is strongly related to the magnitude and phase of SAM. Composites of low-frequency sea surface temperature variation, 200-hPa zonal wind, and outgoing longwave radiation (OLR) indicate that positive (negative) phases of the Southern Annular Mode (SAM) are dominant when patterns of SST, convection, and circulation anomalies resemble the La Niña (El Niño) phase of ENSO, thus ENSO is dynamically linked to SAM (Carvalho et al. 2005).

[8] Interestingly, radiative changes alone are not enough to explain the temperature trends over the WAIS. Regional changes in atmospheric circulation are also required to account for the magnitude of temperature changes seen. These atmospheric circulation changes are likely influencing the SMB as well. This provides motivation to closer examine the role of tropical SST variability (ENSO) and mid to high latitude variability (SAM) in influencing the SMB variations observed in the WAIS firn cores.

4. Data and Methods

[9] This study uses a combination of reanalysis data, models, and ice core data to test the relationship between SMB and synoptic scale modes of climate described in this section. In addition, the statistical methods applied to these data, including direct correlations and composite analysis will be presented.

4.1 Compilation of firn cores

[10] Firn cores are necessary to fill a data gap that exists due to the lack of instrumental data on the Antarctic continent. While firn/ice cores provide excellent temporal records of SMB for a given location, the cores are severely limited spatially as most firn cores are less than 10 cm in diameter. In addition, because of the large degree of small-scale spatial variability found in all Antarctic SMB records, a single core is not representative of region-wide SMB (Burgener, 2012). The spatial limitations of firn cores are compensated for in part by collecting multiple cores in a region and averaging the resulting annual SMB observations together (Genthon et al., 2005). A compact network of SMB consisting of five firn cores from the 2010-2011 SEAT (Satellite Era Accumulation Traverse) field season (Burgener et al., 2013) is expanded with nine ITASE (International Trans Antarctic Scientific Expedition) firn core records (figure 1). A straight stacked record is created from averaging annual SMB for each of the fourteen cores (figure 2). A stacked record eliminates noise and reduces the effects of small scale variability in the record and provides a representation of average regional SMB. Not included in the stack are seven preliminary firn cores from the SEAT 2011-2012 field season as the depth-age scales are not yet finalized.

4.12 Compilation of model/reanalysis data

[11] Due to SMB being a key term in the mass balance equation of an ice sheet, meso-scale model simulations of accumulation across the central region of the WAIS are valuable. These models provide a means of directly linking atmospheric circulation to predicted SMB in a self-consistent way. In other words, these models provide information on the expected SMB variability in response to atmospheric circulation variability that can be compared to the ice core observations. The SEAT 2010 and 14 core stacked records were compared to output of two climate reanalyses generated by the ECMWF (ERA-40 and ERA-interim), two regional climate models (RACMO2.1/ANT and Polar MM5), and NASA's Modern-Era Retrospective Analysis for Research and Applications (MERRA). These models/reanalyses employ different methods for calculating net SMB and differ in spatial resolution (Bromwich et al. 2011). RACMO2.1/ANT uses a complex formula to calculate net SMB that takes into account various ablation processes such as sublimation of blowing snow and horizontal transport. MERRA, ERA-40, ERA-Interim, and Polar MM5 outputs use a simple formula that only accounts for precipitation minus evaporation (P-E). Simulated SMB time series along with the SEAT 2010 stack and 14 core stack are shown in figure 3.

[12] The ERA-40 is a reanalyses of observations from a 45 year period (1957-2002) produced by the European Centre for Medium-Range Weather Forecasts (ECMWF). The ERA-40 provides a number of improvements over the previous ERA-15 including a higher horizontal resolution (2.5 degree latitude x 2.5 degree longitude) and more observations including operational data provided by NCEP and the Japan Meteorological Agency, and in situ and satellite data from NCAR (Uppala et al. 2005). The ERA-interim reanalysis is the latest global atmospheric reanalysis produced by ECMWF, and is the replacement for the ERA-40. This

reanalysis covers the period from January 1979 onwards, and continues to be extended forward in real time. Improvements over the ERA-40 include higher resolution with a 1.5º latitude by 1.5º longitude grid, has better temporal consistency on multiple time scales, and shows better skill at representing the hydrological cycle (Dee et al., 2011).

[13] MERRA is a climate reanalysis developed by NASA with the objectives of placing observations from NASA's Earth Observing System satellites into a climate context and to improve upon the hydrologic cycle as represented in earlier analyses (Reineker et al., 2011). MERRA focuses on the satellite era, from 1979 to the present day and has achieved its goals by significantly improving precipitation and water vapor climatology. MERRA ulililizes the 3DVAR data assimilation analysis algorithm and its resolution is 1/2 º latitude by 2/3 º longitude horizontal grid resolution (Reinker et al., 2011).

[14] Polar MM5 is a regional atmospheric model based on the fifth-generation Pennsylvania State University-National Center for Atmospheric Research (PSU-NCAR) Mesoscale Model, which has been optimized for climate modeling over ice sheets by the Byrd Polar Research Center at the Ohio State University (Bromwich et al., 2004). Polar MM5 covers the period spanning 1979 to 2001. Polar MM5 has a 60km horizontal resolution and its boundary conditions are forced by both ERA-40 and NCEP II (Monaghan et al., 2006b). RACMO2.1/ANT is a regional atmospheric climate model combining the dynamics of the High Resolution Limited Area Model (HIRLAM) and the physical processes of the ECMWF model. RACMO2.1/ANT has been optimized to simulate the climate conditions of large ice sheets. RACMO2.1/ANT covers the period spanning from 1979 to 2010. The model has a horizontal grid spacing of 27 km and is forced at its boundaries by ERA-Interim.

4.2 Climate indices

[15] Indices of SAM and ENSO are used to select the years where each mode of climate was in an extreme positive or negative phase. A climate index is defined as a calculated value that can be used to describe the state and the changes in a climate system. Climate indices are based on certain parameters and describe only certain aspects of climate. Means, extreme values, linear trends, and standard deviations of long time series can be calculated for each of these climate parameters. The climate indices chosen for this study are the SAM index and the Southern Oscillation Index (SOI) (figure 4), both of which are measures of differences in air pressure between two defined locations.

SAM		ENSO	
Positve	Negative	El Nino (Positive)	La Nina (Negative)
2010	2007	2005	2010
2008	2002	2004	2008
2001	1992	2002	2000
1999	1991	1997	1999
1998	1981	1994	1996
1993	1980	1993	1989
1989		1992	1988
1985		1991	1985
1979		1987	1981
		1983	1979
		1982	

Table 1: Extreme negative and positive phase years for SAM and ENSO. An extreme year is defined as any year in the SAM index or SOI that is greater or less than 0.75 standard deviations above/below the mean in the respective index.

[16] The SAM index is defined as the difference of zonal mean sea level pressure between 40ºS and 65ºS (Gong and Wang, 1999). The Southern Oscillation index (SOI), gives an indication of the development and intensity of ENSO events in the Pacific Ocean. The SOI is measured as the difference in sea level pressure between Tahiti and Darwin, Australia. Sustained negative values generally indicate an El Niño episode, where sustained warming of the central

and eastern tropical Pacific and decreased trade winds occur. Sustained positive values generally indicate a La Niña episode, where warmer sea surface temperatures shift to north of Australia and stronger trade winds prevail. From these two indices, mean and standard deviation can be calculated from the detrended data and it is possible to define what the benchmark of an extreme year is for the SAM and ENSO.

4.21 Extreme phases of SAM and ENSO

[17] For this study an extreme year will be defined as any year where an index (SAM Index or SOI) value is >0.75 standard deviations above the mean or <0.75 standard deviations below the mean. The value of 0.75 standard deviations was chosen to capture a representative portion of the each phase of SAM and ENSO. While there is no real cutoff for the acceptable amount of years to be included for each phase of SAM and ENSO, it is important to have a large enough sample size that is representative of each possible case. For the SAM index, any year >0.75 standard deviations above the mean is considered an extreme positive phase and any year <0.75 standard deviations below the mean is considered an extreme negative phase. For the SOI, any year that is >0.75 standard deviations above the mean is considered an extreme negative phase (La Niña) and any year <0.75 standard deviations below the mean is considered an extreme positive phase (El Niño). Presented in table 1 are all years that qualified as extreme for both SAM and ENSO. These identified years where SAM and ESNO were in an extreme phase will be used to calculate SMB and atmospheric circulation anomalies.

4.3 Direct correlations between synoptic scale modes of climate and SMB

[18] To test the strength and direction of the linear relationship between SAM, ENSO, and WAIS SMB, a matrix is created by correlating all combinations of SMB and climate index data. Two annual stacked SMB records are used to represent regional SMB over the WAIS: The SEAT 2010 stack, which consists of five high resolution firn core records, and the 14 core regional stack, which is a combination of the five SEAT 2010 firn cores and nine ITASE firn cores. The SAM is represented by the SAM index, and ENSO is represented by the SOI. All of the aforementioned data covers the 32 year period, 1979-2010. The correlation coefficient (r) and accompanying p-value is calculated between each combination of climate index and SMB. While correlation is a useful indicator of the strength and direction of the linear relationship between two data sets, it does not address why a relationship is poor or strong, the mechanisms giving rise to that relationship.

5. Results and Conclusions

[19] This section presents the results of the statistical tests used to assess the relationship between synoptic scale modes of climate and SMB records. This includes the direct correlation between SMB records and synoptic scale modes of climate, and composite analysis comparing SMB, mslp and Z_{200} data during extreme years of SAM and ENSO to average. Lastly, the statistical significance of the resulting correlations and anomalies are presented in this section.

5.1 Direct correlation between SMB and synoptic scale modes of climate

[20] The direct correlation between synoptic scale modes of climate and Antarctic SMB is poor (table 2). The highest statistically significant correlation is between the SOI and the SMB records, but only account for 22% of the variance. Importantly, the correlation with SAM is not statistically significant. These results could be due to the influence tropical SST forcing has on

the SAM (Fogt and Bromwich, 2006; Ding and Steig, 2012). A poor correlation could be due to many circulation patterns giving rise to average SMB in any given year or dating uncertainties in reconstructed firn core records. If there is an influence of synoptic scale modes of climate on WAIS SMB, the impact should at least be observed in the extreme years of SAM and/or ENSO. Therefore, composite analysis is used to assess the influences of SAM and ENSO on WAIS SMB and atmospheric circulation patterns during the extreme years.

	SAM	SOI
SEAT 2010	0.15	0.47
Stack	0.24	0.42

	SAM	SOI
SEAT 2010	0.406	0.006
Stack	0.174	0.014

Table 2: a. Correlation Matrix showing correlation of SAM (SAM Index) and ENSO (SOI) against stacked records. Overall correlation is low between large scale climate variability and the annual accumulation records. b. P-values from testing the significance of r values in the correlation matrix. P-values in red are significant at the 95% confidence level.

5.2 Composite Analysis of SMB during extreme years of SAM and ENSO

[21] Annual SMB from 5 models/reanalyses and a straight stack of 14 SEAT and seven ITASE cores are used to compare SMB during extreme years of SAM and ENSO to the average of all years. To calculate the anomaly for each scenario, the average SMB for a particular phase of either SAM or ENSO (ex: All extreme positive SAM years) is subtracted from the mean SMB from the period 1979-2011. Table 3 (part a) contains the anomalies for the positive and negative phase of SAM and ENSO for each model/reanalyses and the stacked record. The anomalies show that during the negative phases of SAM and ENSO, there is a slight increase in annual accumulation for all models/reanalyses and the stacked record. During extreme positive ENSO (El Niño) years, the anomalies range from 0.82 to 1.56 w.e. cm/yr above the mean on average, while the anomalies during extreme negative SAM years ranged from 0.56 to 3.41 w.e. cm/yr above the mean on average. During extreme negative ENSO (La Niña) years, the anomalies range from 0.37 to 1.26 w.e. cm/yr below the mean on average, while during extreme positive

SAM years, anomalies ranged from 0.30 to 1.20 w.e cm/yr below the mean on average. These anomalies suggest that certain extreme phases of SAM or ENSO produce lower than average SMB over the central WAIS, but statistical testing is necessary to determine whether the calculated differences are significantly different from the mean.

a. Climate Indice	Phase	ERA-40	ERA-interim	MERRA	Polar MM5	RACMO	14 core stack
SOI	*El Niño*	0.97	1.56	1.17	1.09	0.82	1.32
	La Niña	-0.44	-1.17	-0.68	-1.26	-0.36	-0.37
SAM Index	*Positive*	-0.43	-1.20	-0.30	-0.56	-0.50	-0.80
	Negative	2.64	3.04	1.69	3.41	2.01	0.56

b. Climate Indice	Phase	ERA-40	ERA-interim	MERRA	Polar MM5	RACMO	14 core stack
SOI	*El Niño*	0.0096	0.0011	0.0004	0.1143	0.0010	0.1585
	La Niña	0.0014	0.0008	0.0017	0.0005	0.0011	0.0381
SAM Index	*Positive*	0.0389	0.0189	0.0436	0.0257	0.0395	0.0453
	Negative	0.0496	0.0071	0.0380	0.0553	0.0376	0.1690

Table 3: a) Annual SMB anomalies (w.e. cm/yr) for five models/reanalyses and a 19 core stacked record for the extreme years of SAM and ENSO. The five simulated records and the stacked record anomalies show that annual accumulation during extreme negative (positive) years of SAM and positive (negative) years of ENSO are higher (lower) than average. b) A two sample Welch's t-test was performed comparing accumulation during extreme years to all other years. The differences are significant ($p<0.05$) for all scenarios but three (PMM5 El Nino anomaly, and stacked record anomalies for positive and negative phases of SAM).

[22] A two sample Welch's t-test was performed to compare SMB during years where SAM/ENSO are extremely negative/positive to annual accumulation for all years with a null hypothesis stating there is no significant difference between the extreme years and average SMB. Table 3 (part b) contains the p-values for each combination of phase and simulated/actual SMB. The p-values show that a majority of the possible combinations are statistically significant at the 95% confidence level. So while the anomalies are not necessarily large at first glance, the difference from the mean during extreme years of SAM/ENSO are suggested by the data to be for the most part significantly different from the mean. Snow accumulation is the only way mass is added to the WAIS, so even small changes over space and time can lead to significant changes

in mass on the ice sheet. The key result of the statistical testing is the significance of the anomalies during the extreme positive phase of SAM and the negative phase of ESNO. The anomalies for all cases (simulated and actual SMB) during these two phases are statistically significant at the 95% confidence level, suggesting that the lower than average SMB during these two extreme phases is significantly different from the mean. These anomalies suggest that the phase of SAM or ENSO plays an important role in contributing to SMB variability over the WAIS. To validate these results, it is necessary to examine atmospheric circulation anomalies to better understand the circulation patterns that accompany SAM and ENSO.

5.3 Atmospheric anomalies during extreme years of SAM and ENSO

[23] Annual and seasonal atmospheric anomaly plots are created to show the circulation patterns that occur at the surface and high above the surface during a particular phase of SAM or ENSO. Mean sea level pressure (mslp) anomalies and 200-hPa Z_{200} geopotential height anomalies were collected from the ERA-interim from the period 1979-2011. 200-hPa geopotential heights Z_{200} are used because 200 hPa corresponds to the core of the tropospheric jet stream (Ding and Steig, 2012), while mslp is used to allow comparison of circulation anomalies at the surface and troposphere. A two sample t-test was performed on the imported data to test whether the plotted anomalies were significantly different from the mean at the 95% confidence level. Significance is represented on each plot with a small black dot for each grid point where the anomaly is significantly different from the mean.

5.31 Mean annual anomalies

[24] Mean sea level pressure (mslp) and Z_{200} anomalies are based off SAM extreme years, SOI extreme years, and anomalously high/low SMB years from the stacked record consisting of 14 SEAT and ITASE cores. The annual mslp (figure 5) and Z_{200} (figure 6) anomaly plots show a persistent area of low pressure off the coast of West Antarctica over the Amundsen Sea during the positive phase of SAM, the negative phase of ENSO, and the years of anomalously low SMB from the stacked record. The low pressure anomalies in all three plots are statistically significant at the 95% confidence level. The location of the low in all three plots would put the Antarctic Peninsula (AP) in a position to receive higher than average SMB, while the WAIS interior is in a position to receive lower than average SMB (figure 9). The results strongly suggest that the low pressure anomaly associated with the positive phase of SAM and the negative phase of ENSO drives anomalously low precipitation in central WAIS.

[25] The extreme positive phase of ENSO and the extreme negative phase of SAM show an area of high pressure over the Amundsen Sea with low pressure cells positioned around the rest of the Antarctic continent. This pattern is reminiscent of a Rossby wave train, which is a series of high and low pressure cells that follow an arcing path from the tropical pacific to WA. This pattern is known to produce warming westerly winds over WA due to the area of high pressure that is positioned over the Amundsen Sea (Ding et al., 2011). The mean annual anomalies representing years of high SMB from the stacked record is significantly different than either phase of SAM and ENSO, with a significant low anomaly centered between the Amundsen and Ross seas. Additionally, this low is positioned over the Amundsen Sea in the mslp anomaly plot and over the Ross Sea ice shelf the Z_{200} plot. This offset gives rise to baroclinic instability, which drives the generation of cyclones that are steered by the upper

atmospheric winds into western and central WAIS. The mslp and Z_{200} annual plots suggest that there are at least two patterns that can drive higher than average SMB over WA.

[26] A high pressure anomaly over the Amundsen Sea, or a shift of the low pressure system and upper level winds over the Ross Sea are the dominant patterns that drive SMB variability over the central WAIS. The seasonal anomaly plots will reveal shifts in circulation patterns from season to season.

5.32 Extreme positive phase of SAM

[27] The mslp and Z_{200} anomalies show seasonal circulation patterns that are associated with the extreme positive phase of SAM (Figures 7 and 8). The dominant feature is a persistent area of low pressure centered off the coast of WA over the Amundsen Sea. This low persists over all seasons, with small variations in location and strength from season to season. The low is statistically different from the mean during austral autumn and winter. This pattern shows the circumpolar vortex, the belt of tropospheric westerlies, weakens and contracts towards Antarctica when SAM is positive (Naik et al., 2010). This results in cooling over much of East Antarctica, with WA being the exception. Under this particular flow regime (figure 9), low pressure over the Amundsen Sea induces lower than average SMB over western WA, with increased westerlies, warming, and higher than average SMB over the Antarctic Peninsula (AP) due to moisture advection changes (Genthon, 2005).

5.33 Extreme negative phase of SAM

[28] During the extreme negative phase of SAM, the persistent low is replaced by an area of high pressure in almost the same location, which is evident during austral autumn and winter. There is greater heat exchange between the tropics and the poles with the circumpolar vortex strengthening, resulting in an anticyclonic anomaly over the Amundsen-Bellingshausen Sea

(Turner, 2004). High pressure over the Amundsen Sea with three low pressure anomalies surrounding the rest of the Antarctic continent, resembling a Rossby wave, is evident in the seasonal mlsp (figure 10) and Z_{200} (figure 11) anomalies. The pattern is most evident during austral winter and spring, with nearly all of the anomalous high and low centers being significant during this period. The largest deviation between the two extreme phases of SAM is that the negative phase leads to a greater amount of variability from season to season while the positive phase produces a fairly consistent pattern to set up over WA. The distinct circulation patterns that accompany both phases of SAM are capable of bringing anomalous accumulation to the central WAIS, contributing to the observed variability. With a good idea of what circulation patterns accompany SAM, plotting anomalies during years of anomalously low/high SMB from the stacked record will reveal what circulation patterns give rise to extreme accumulation events over the central WAIS.

5.34 Anomalously low SMB years from stacked record

[29] During years where SMB in the stacked record is anomalously low, the mslp (figure 12) and Z_{200} (figure 13) seasonal anomalies largely mimic the circulation patterns observed during the positive phase of SAM. While the match is not perfect, there is a statistically significant persistent area of low pressure off the coast of WA over all seasons, with a high pressure anomaly over most of Eastern Antarctica during all seasons except austral spring. This low shifts around from season to season, with the low moving closer to the Ross Sea during austral winter and moving over the Bellingshausen Sea near the AP during austral spring. The change from season to season is minimal, which is quite similar to the extreme positive phase of SAM seasonal anomaly plots. While there appears to be a limited number of circulation patterns

that give rise to below average SMB over the central WAIS, this does not hold true for years of anomalously high SMB from the stacked record.

5.35 Anomalously high SMB years from stacked record

[30] While the seasonal anomalies during anomalously low SMB years from the stacked record mimicked the positive phase of SAM, the seasonal anomalies from the years of anomalously high SMB from the stacked record do not mimic any patterns observed during either extreme phase of SAM. There is nearly no continuity from season to season with many different patterns that could influence SMB visible in the mslp (figure 14) and Z_{200} (figure 15) seasonal anomalies. The most prominent circulation pattern that appears is an area of low pressure over the Ross Sea during austral spring and autumn. The positioning of this low would place the central WAIS in position to receive higher than average SMB. The lack of any persistent pattern indicates that there are a greater combination of circulation patterns that can contribute to higher SMB over the central WAIS. The anomaly plots provide important evidence linking circulation patterns associated with phases of SAM and ENSO to WAIS SMB variability.

5.4 Conclusions

[31] Previous studies have linked both tropical (ENSO) and mid-latitude (SAM) synoptic scale modes of climate to southern hemisphere internal climate variability. Since the 1970's, a positive trend in the SAM index has led to persistent low pressure over the Amundsen Sea, which is thought to be a factor in contributing to WAIS SMB variability. While SAM and ENSO tend to be viewed as independently driving circulation, temperature, and precipitation changes in the southern hemisphere, there is evidence supporting that mid to high latitude climate variability is connected to variability in the tropics. ENSO has been known to interact with SAM with changes occurring in the tropics due to ENSO have a ripple effect in the high latitudes (Fogt et

al., 2011). Synoptic scale modes of climate are believed to be contributors to the SMB variability but the assumption has not been rigorously tested.

[32] With a low direct correlation between SAM, ENSO, and ice core records, the years where SAM and ENSO were in an extreme phase were studied with the hypothesis that these extreme phases are leading to circulation patterns that contribute to the variability of the WAIS SMB. This study performed a composite analysis using ice core data and climate indices to assess how synoptic scale modes of climate contribute to SMB variability on the WAIS. Statistically significant SMB anomalies reveal that below average SMB occurs when SAM was extremely positive or ENSO was extremely negative. Conversely, statistically significant SMB anomalies during the years where SAM was extremely negative or ENSO was extremely positive produced above average SMB over central WAIS, although there were a few scenarios where the difference from the mean was not statistically significant. A composite analysis was also performed on annual and seasonal mslp and Z_{200} atmospheric data over the SH. The anomalies were tested for statistical significance using a two-sample t test at the 95% confidence level. The annual and seasonal anomalies were plotted, showing circulation patterns that occur during the extreme phases of SAM, ESNO, and anomalously high/low SMB from the stacked record.

[33] The annual and seasonal anomalies show a persistent area of low pressure that is positioned over the Amundsen Sea when SAM is in an extreme positive phase or ENSO is in an extreme negative phase. This circulation pattern gives rise to lower than average SMB over Western WAIS and higher SMB over the AP. This pattern is important as SAM has been shifting towards the positive phase with greater frequency over the past few decades (Sigmond et al., 2010). Seasonal plots focusing on anomalously low years of SMB from the regional 14 core

stacked record show similar circulation patterns observed during the negative phase of ENSO and the positive phase of SAM, with persistent low pressure over the Amundsen Sea.

[34] When SAM is in an extreme negative phase, the tropospheric belt of westerlies (circumpolar vortex) strengthen and the pattern around Antarctica resembles a Rossby wave train, with high pressure positioned over the Amundsen Sea during austral autumn and winter. This pattern supports strengthening westerlies and warming over WAIS with the potential for higher than average SMB. However, while there is a tendency towards increased SMB during the negative phase of SAM, higher SMB is also highly likely when the mslp and Z_{200} low shifts towards the Ross Sea. Therefore, while low SMB has a direct relationship with SAM and ENSO, average to high SMB does not. This is the likely cause of the low direct correlation between the climate indices and SMB.

[35] The results suggest that the best predictor for extreme accumulation events is the geographical location of regional low and high pressure systems, and not solely the intensity of the low pressure systems as has been previously assumed. There is significant evidence that synoptic scale modes of climate contribute to observed SMB variability on the WAIS. As seen in the anomaly plots, the location of regional low and high pressure systems is tied to circulation patterns that accompany a particular phase of SAM or ENSO, though the relationship is complicated. In any given year, the phase of SAM or ENSO will play a role in the circulation patterns that develop over the high latitudes and regulate the geographical positioning of low and high pressure systems, which will contribute to the SMB variability over the WAIS. These results have direct implications for paleoclimate reconstructions from ice core data, climate model validation, ice sheet modeling, and the future evolution of the WAIS SMB.

Part 2: Temporal trends

6. Introduction to temporal trends

[36] There is significant evidence that synoptic scale modes of climate do influence SMB in central WAIS, though not in a simple way (Part I). In recent decades, trend of atmospheric circulation toward the positive phase of SAM has been observed, manifested as a strengthening of the circumpolar westerlies along 60ºS, which has been attributed to both increased greenhouse gas concentrations and stratospheric ozone depletion (Thompson and Solomon 2002, Ding and Steig 2012, Marshall, 2007). The extreme positive phase of SAM has been shown in this study to consistently produce circulation patterns that results in lower than average SMB over the central WAIS. Given the results in this study, there might be an expectation that this has given rise to a decrease in SMB over the WAIS interior. Five firn cores drilled during the 2010 field season (Burgener et al., 2013) show a significant decline in SMB over the past three decades, but these firn cores are spatially limited. If the trend towards the positive phase of SAM is driving the trend in negative SMB, then the impacts should extend to a larger area.

[37] This study expands the compact network of high temporal resolution firn cores by adding seven new high temporal resolution firn cores extracted from an adjacent region on the WAIS interior during the 2011-2012 Antarctic field season (table 4). The first five firn cores from the 2010-2011 field season filled a temporal and spatial gap in the central WAIS region. The new suite of cores provide new data critical for showing recent region-wide trends in SMB. These new firn cores aid the existing cores in overcoming small scale spatial variability and providing a more accurate representation of regional SMB over the past three decades. Second, with a larger pool of data to work from, a suite of statistical analyses can be performed to test the

significance of the observed trends from the firn core records and produce a regional representation of how SMB has been changing in the past few decades.

Core Name	Latitude (N)	Longitude (E)	Elevation (m)	Age Range (Years)
SEAT 10-1	-79.383	-111.239	1790.7	1976-2010
SEAT 10-2	-79.407	-111.654	1171.8	NA
SEAT 10-3	-79.042	-111.547	1771.8	1975-2010
SEAT 10-4	-78.488	-111.698	1649.8	1970-2010
SEAT 10-5	-79.123	-113.041	1793.7	1978-2010
SEAT 10-6	-79.751	-114.552	1693.6	1966-2010
SEAT 11-1	-80.009	-119.423	1502.9	1982-2011
SEAT 11-2	-79.348	-116.29	1681.1	1981-2011
SEAT 11-3	-78.728	-114.732	1782.7	1980-2011
SEAT 11-4	-78.311	-113.788	1608.7	1986-2011
SEAT 11-5	-78.312	-113.793	1610.1	NA
SEAT 11-6	-78.424	-115.292	1731	1986-2011
SEAT 11-7	-78.837	-116.307	1739.4	1977-2011
SEAT 11-8	-79.447	-117.963	1618.5	1977-2011
SEAT 11-9	-79.446	-117.969	1618.4	NA

Table 4: SEAT ice cores extracted between the 2010 and 2011 field seasons.

7. Methods

7.1 Field Methods

[38] The 2010-2011 Satellite Era Accumulation Traverse (SEAT) was conducted by a six person team traveling from the WAIS Divide Deep Core Camp. Five cores were collected at sites ~70km apart, ranging across the ice divide. In 2011, nine additional cores were drilled in the same area (this study), creating a region wide spatial network of fourteen new shallow firn cores (Figure 1).

[39] At each drilling location, a snow pit was dug through the top layers of snow and firn until a depth was reached where the firn was dense enough to remain intact during drilling, which according to (Burgener et al., 2013) was ~1.5 meters. Density measurements for the snow

pit samples were performed at every 2 cm. The firn core sections generally measured ~80 cm from the bottom of the snow pit at each drilling site. Due to the youngest firn being poorly compacted at several sites, the upper 1 to 2 meters was samples in the field. Each core section was measured for bulk weight and length, which later was used for firn density calculations. The sampling process included electrical conductivity measurements (ECM) for each core section, with the sections being cut into ~2 cm samples. Volume and mass measurements were then taken and recorded for every sample. The procedure for the SEAT 2011 cores remained similar to that of the previous year with minor exceptions. To increase efficiency of the drilling operations, the core was drilled next to the pit wall (Williams et al., 2013).

7.2 Lab Methods

[40] The core sections and snow pit samples were shipped in large insulated boxes to the Climate Dynamics Lab at Brigham Young University in Provo, Utah. Temperatures were maintained at -20 degrees Celsius throughout transit. The ice cores and snow pit samples were stored and processed in a walk in freezer in the Climate Dynamics Lab, where the freezer temperature generally varied between -15 and -30 degrees Celsius. The core sections were processed from top (near surface) to bottom for each core as the sample numbers from each core began at the top and finished at the bottom. Each core was weighed and measured to ensure measurements taken in the field were accurate, and to assess the loss of snow on transit. The core was then placed beneath a fluorescent light where the cool bulb revealed the stratigraphy of the firn core sections, revealing seasonal layers, wind layers, and hoar frost layers. Any interesting features of the firn core sections were recorded and high resolution pictures of the stratigraphy were taken of each section. The core section was then cut into approximately two centimeter samples. Volume measurements were promptly taken for each two centimeter section using

digital calipers, with the thickness and width being taken three times and then recorded by a scribe.

[41] After the volume measurements were completed, each sample was bagged in a whirl pak sample bag. Samples were placed in a cooler and the samples from each section were weighed three times. The volume and density calculations after being entered into excel were used to calculate density for each sample and cumulatively for each firn core. Cumulative uncertainties for the density calculations are 10% for snowpit samples and 5% for firn core samples. The average volume measurement (cm^3) is multiplied by the average weight of each sample (in grams), providing a slice by slice density through the length of the whole firn core.

[42] Samples were then stored in the freezer until ready to be melted and decanted. To minimize any isotopic shifts during processing, great care was taken. The samples were double bagged and hung on a clothesline, and allowed to melt at room temperature (~22 degrees C). Once the samples were in a liquid state, they were immediately decanted from the sample bag into pre-labeled 20 mL Nalgene bottles with corresponding sample numbers. The bottles were sealed tightly to prevent any isotopic interaction between the sample and the atmosphere and then frozen until ready for further processing.

[43] Isotopic analysis ($\delta^{18}O$ and δD) of the liquid samples was conducted using a Los Gatos Liquid Water Isotope Analyzer (LWIA-24d). Batch sample set up followed the procedure outlined in Nelson (2000) and Nelson and Dettman (2001). A small amount (0.7mL) of each sample was injected into a vial using a pipette and capped to prevent exchange with the atmosphere. The vials were loaded into a tray and samples were run with the liquid isotopic analyzer taking eight injections from each vial. Memory correction was addressed by rejecting the first four injections for each sample. The next four injections for each sample were then drift

corrected using in house standards (the procedure used was taken from Nelson and Dettman, 2001). The in house standards (calibrated by Vienna Standard Mean Ocean Water and Standard Light Antarctic Precipitation) have isotopic values that are within the range of the SEAT isotopic data, thus reducing the influence of memory. In addition to the aforementioned two standards, a quality check sample of similar isotopic values to the WAIS samples (Steig et al., 2013) was used to determine the error in the drift corrected samples all through a batch. The final isotopic composition of a sample was determined by taking the average of the drift corrected injections (Williams et al., 2013). The analytical uncertainties are 0.6 ‰ for $\delta^{18}O$ and 0.2‰ for δD.

[44] Water-equivalent annual SMB records were created using both the density profiles and depth-age scales. Depth-age scales at seasonal resolution were created for each core by counting the peaks and troughs in the seasonal signal of the δ18O and δD records. These first and preliminary depth-age scales were refined and verified by comparing the isotopic profiles to the density profiles and solute concentrations in each core. The solute data was measured using a Dionex ICS-90 Ion Chromatography System. Solute data provides definite years in the firn core records and serves as a refining tool for the depth age scales. Solute data is still in progress for the SEAT 2011 firn cores, thus the new accumulation records (this study) are still considered preliminary. The records were reconstructed by multiplying the density of each sample by its respective thickness and then summing up all samples that belonged to a particular year, according to the method described in Cuffey and Paterson (2010).

8. Results and Discussion: Trends observed in the SEAT 2010 and 2011 firn core records

[45] The trends in the preliminary SEAT-2011 reconstructed firn core records will analyzed and compared with the existing SEAT-2010 records. The observed trends in these firn cores are similar in magnitude and sign as the SEAT-2010 cores, then this will be indicative of a

regional trend that is likely connected atmospheric circulation patterns associated with synoptic scale modes of climate. Additionally, the statistical significance of the observed temporal trends will be presented in this section.

8.1 SEAT-2010 and SEAT-2011 SMB Rate

[46] Figure 16 shows the reconstructed annual SMB for the five SEAT-2010 firn cores collected during the SEAT 2010-2011 field season. The records from each core cover different timespans with the longest record (SEAT 10-6) extending back to 1966 and the shortest (SEAT 10-5) extending back to 1976 (Burgener et al., 2013). The trends from each of the SEAT-2010 cores show a statistically significant decreasing trend in SMB, ranging from a maximum decrease of -7.2 cm to a minimum of -1.5 cm w.e per decade.

Core Name	Max	Mean	Min	Median	StDev	Variance	Skewness	Kurtosis
SEAT 10-1	33.535	21.498	12.653	21.548	5.382	28.965	0.127	-0.614
SEAT 10-3	49.073	21.266	8.152	19.182	9.319	86.849	0.696	0.363
SEAT 10-4	57.694	27.991	6.157	24.666	13.803	190.516	0.451	-0.848
SEAT 10-5	40.911	23.982	6.926	25.416	7.567	57.257	-0.543	0.302
SEAT 10-6	36.741	20.469	10.279	18.047	7.466	55.745	0.677	-0.475
SEAT 11-1	53.632	26.419	9.791	24.573	12.466	155.397	0.660	-0.614
SEAT 11-2	63.487	31.062	7.707	29.673	14.877	221.330	0.436	-0.622
SEAT 11-3	46.411	28.798	8.375	28.905	8.600	73.954	-0.351	0.283
SEAT 11-4	59.310	36.061	6.741	40.900	14.734	217.076	-0.507	-0.745
SEAT 11-6	58.645	35.783	7.115	41.640	14.561	212.024	-0.519	-0.799
SEAT 11-7	50.318	25.516	8.956	22.267	11.562	133.690	0.619	-0.597
SEAT 11-8	64.190	31.085	10.747	29.932	13.397	179.466	0.479	-0.262

Table 5: Simple statistical data for annual accumulation (w.e. cm/yr) data reconstructed from the SEAT 2010 and 2011 firn cores. The preliminary SEAT 2011 cores in general have higher accumulation rates due to closer proximity to the coast.

[47] Figure 17 shows the reconstructed preliminary SEAT-2011 SMB records. The SEAT-2011 cores also show negative SMB trends. The records from each core vary in their temporal length, with the longest two records (SEAT 11-7 and SEAT 11-8) spanning from 1977-2011, and the shortest two (SEAT 11-4 and SEAT 11-6) spanning from 1986-2011. In general

the SEAT-2011 temporal records are shorter than the SEAT 2010 records as shown in table 4. The SEAT-2011 records generally show higher mean SMB than what is observed in the SEAT-2010 records, which can be explained by closer proximity to the coast (figure 18), which is in general agreement with previous studies (Kaspari et al., 2004). In addition to mean SMB, additional simple statistical relationships were established for each SMB record (table 5).The trends from each of the SEAT-2011 cores show a statistically significant decreasing trend in SMB, ranging from a maximum decrease of -10.05 cm to a minimum of -1.15 cm w.e per decade. These trends are the same magnitude as the SEAT 2010 firn cores. The statistical significance of these trends will be discussed further in depth in the next section.

8.2 Statistical Analysis of Temporal Trends

[48] Statistical testing is performed on the records to improve understanding of whether the observations in the records are significant. In order to evaluate the significance of the SEAT 2010 and 2011 SMB trends, stacked SMB records are used. Spatially averaging a number of SMB records together acts to reduce the amount of small scale perturbations (SSP), which can be noise due to wind redistribution, sublimation, etc. (Genthon et al., 2005). Two stacks are created, the first consisting of the five SEAT-2010 firn cores and the second consisting of the seven preliminary SEAT-2011 firn cores (figure 19). The stacks are created by averaging SMB between all cores in the stack for each year.

[49] In order to determine the significance of the SMB trends, an ordinary least squares (OLS) regression model was fit to each of the five SEAT 2010, seven SEAT 2011 and the two stacked SMB records. Table 6 shows the resulting statistics and p-values for each of the records. Both the individual and stacked records show a significant negative trends in SMB for the length of each record. All but one of the records (SEAT 10-5) are significant when considering the

period of 1980-2010, and a majority of the records are significant from the period 1990-2010. The results from the period of 1990-2010 are not considered as reliable due to the smaller sampling size. Regardless, the results suggest that the observed decrease in annual SMB in all SEAT cores is likely a regional trend and not due to noise from within the system. The declining regional trend supports the composite analysis in part 1 of this study which showed that certain circulation patterns that gave rise to decreased SMB over the central WAIS were associated with the extreme positive phase of SAM or the extreme negative phase of ENSO.

a.

Core/Period	Time Period	OLS Model	
		t-statistic	p-value
SEAT 10 Stack	1976-2010	-6.96	<0.0001
SEAT-10-1	1976-2010	-2.69	0.0109
SEAT-10-3	1975-2010	-4.52	<0.0001
SEAT-10-4	1968-2010	-5.17	<0.0001
SEAT-10-5	1978-2010	-2.14	0.0402
SEAT-10-6	1966-2010	-3.21	0.0025

b.

Core/Period	Time Period	OLS Model	
		t-statistic	p-value
SEAT 11 Stack	1977-2010	-4.60	0.0001
SEAT-11-1	1982-2011	-4.29	0.0002
SEAT-11-2	1981-2011	-5.59	<0.0001
SEAT-11-3	1980-2011	-5.59	<0.0001
SEAT-11-4	1986-2011	-2.81	0.0098
SEAT-11-6	1986-2011	-2.95	0.0073
SEAT-11-7	1977-2010	-3.77	0.0008
SEAT-11-8	1977-2010	-4.24	0.0002

Table 6: Statistical significance of accumulation trends for a) SEAT 2010 individual firn cores and stacked record and b) SEAT 2011 individual firn cores and stacked record. All p-values are significant at the 95% confidence level.

9. Conclusions

[50] The addition of seven new reconstructed firn core records to existing records continue to show a region wide decreasing trend in SMB. This trend is not expected as Western Antarctica is warming, which would lead to the expectation of increased precipitation over the WAIS interior. The decreasing SMB trend observed in the new cores are of similar magnitude as the SEAT 2010 cores. Statistical analysis shows that the negative trend is statistically significant at the 95% confidence interval for all twelve SEAT cores and the stacked record.

[51] The decrease in the SEAT cores cannot be easily explained by regional influences, such as temperature, topography, or sea ice extent. No clear trends exist in temperature in the

isotopic records, which rules out temperature being a significant contributor in the past three decades to the decreasing SMB trend. Topography of the SEAT cores lack large surface slopes of undulations that could contribute to what is being observed in the records (Burgener et al. 2013). This suggests that small scale variability is likely not significant contributor to the observed trends in the individual cores. It is likely that synoptic scale climate variability in the tropics and mid to high latitudes are contributing to the observed trends in the firn core records.

[52] If synoptic scale modes of climate are a significant contributor to changing circulation patterns in the southern hemisphere, then future SMB will likely be strongly tied to what phase SAM and ESNO are in. Given the link between ENSO and SMB, any trends in ENSO will directly influence central WAIS SMB. In addition, recent warming has been explained in part by a positive trend in the SAM, which is attributed to stratospheric ozone depletion and increasing greenhouse gases (Ding et al., 2011). If SAM continues to trend more towards the positive phase, it is expected that circulation patterns that are conducive for below average snowfall and warming over the WAIS interior will become more frequent and persistent. This will not only contribute to further mass loss over the WAIS interior, but strongly influence climate over all of West Antarctica.

10. References Cited

Banta, J.R., Mcconnell, J.R., Frey, M.M., Bales, R.C., and Taylor, K., 2008, Spatial and temporal variability in snow accumulation at the West Antarctic Ice Sheet Divide over recent centuries: Journal of Geophysical Research: Atmospheres, v. 113.

Bromwich, D.H., and Fogt, R.L., 2004, Strong trends in the skill of the ERA-40 and NCEP-NCAR Reanalyses in the high and midlatitudes of the Southern Hemisphere, 1958-2001: Journal of Climate, v. 17, p. 4603-4619.

Burgener, L.K., 2012, Temporal trends in west antarctic accumulation rates : evidence from observed and simulated records: Thesis (Master of Science)-Brigham Young University. Department of Geological Sciences, 2012.

Burgener, L., Rupper, S., Koenig, L., Forster, R., Christensen, W.F., Williams, J., Koutnik, M., Miège, C., Steig, E.J., Tingey, D., Keeler, D., and Riley, L., 2013, An observed negative trend in West Antarctic accumulation rates from 1975 to 2010: Evidence from new observed and simulated records: Journal of Geophysical Research: Atmospheres, v. 118, p. 4205-4216.

Carvalho, L., Jones, C., and Ambrizzi, T., 2005, Opposite phases of the antarctic oscillation and relationships with intraseasonal to interannual activity in the tropics during the austral summer: Journal of Climate, v. 18, p. 702-718.

Cuffey, K., and Paterson, W.S.B., 2010, The physics of glaciers, 4th ed. Burlington, MA, Butterworth-Heinemann, p. 693.

Cullather, R., Bromwich, D., and VanWoert, M., 1996, Interannual variations in Antarctic precipitation related to El Nino southern oscillation: Journal of Geophysical Research-Atmospheres, v. 101, p. 19109-19118.

Dee, D.P., Uppala, S.M., Simmons, A.J., Berrisford, P., Poli, P., Kobayashi, S., Andrae, U., Balmaseda, M.A., Balsamo, G., Bauer, P., Bechtold, P., Beljaars, A.C.M., van de berg, L., Bidlot, J., Bormann, N., Delsol, C., Dragani, R., Fuentes, M., Geer, A.J., Haimberger, L., Healy, S.B., Hersbach, H., Holm, E.V., and Isaksen, L., 2011, The ERA-Interim reanalysis: configuration and performance of the data assimilation system: Quarterly Journal of the Royal Meteorological Society, v. 137, p. 553-597.

Ding, Qinghua; Steig, Eric J.; Battisti, David S.; Küttel, Marcel (2011). "Winter warming in West Antarctica caused by central tropical Pacific warming". Nature Geoscience, v.4 (6): 398.

Dinniman, M.S., Klinck, J.M., and Smith, W.O., 2011, A model study of Circumpolar Deep Water on the West Antarctic Peninsula and Ross Sea continental shelves: Deep-Sea Research Part II, v. 58, p. 1508-1523.

Eisen, O., Frezzotti, M., Genthon, C., Isaksson, E., Magand, O., van den Broeke, M., Dixon, D., Ekaykin, A., Holmlund, P., Kameda, T., Karlof, L., Kaspari, S., Lipenkov, V., Oerter, H., Takahashi, S., and Vaughan, D., 2008, Ground-based measurements of spatial and temporal variability of snow accumulation in east Antarctica: Reviews of Geophysics, v. 46.

Frezzotti, M., Urbini, S., Proposito, M., Scarchilli, C., and Gandolfi, S., 2007, Spatial and temporal variability of surface mass balance near Talos Dome, East Antarctica: Journal of Geophysical Research: Earth Surface, v. 112.

Frezzotti, M., Urbini, S., Proposito, M., Scarchilli, C., and Gandolfi, S., 2007, Spatial and temporal variability of surface mass balance near Talos Dome, East Antarctica: Journal of Geophysical Research: Earth Surface, v. 112.

Fogt, R., Bromwich, D., and Hines, K., 2011, Understanding the SAM influence on the South Pacific ENSO teleconnection: Climate Dynamics, v. 36, p. 1555-1576.

Genthon, C., Kaspari, S., and Mayewski, P., 2005, Interannual variability of the surface mass balance of West Antarctica from ITASE cores and ERA40 reanalyses, 1958–2000: Climate Dynamics, v. 24, p. 759-770.

Genthon, C., Krinner, G., and Sacchettini, M., 2003, Interannual Antarctic tropospheric circulation and precipitation variability: Climate Dynamics, v. 21, p. 289-307.

Gong, D., and Wang, S., 1999, Definition of Antarctic Oscillation index: Geophysical Research Letters, v. 26, p. 459-462.

Kwok, R., and Comiso, J.C., 2002, Spatial patterns of variability in Antarctic surface temperature: Connections to the Southern Hemisphere Annular Mode and the Southern Oscillation: Geophysical Research Letters, v. 29.

Lenaerts, J.T.M., Den Broeke, M.R., Berg, W.J., Meijgaard, E., and Kuipers Munneke, P., 2012, A new, high-resolution surface mass balance map of Antarctica (1979–2010) based on regional atmospheric climate modeling: Geophysical Research Letters, v. 39.

Marshall, G., Di Battista, S., Naik, S., and Thamban, M., 2011, Analysis of a regional change in the sign of the SAM-temperature relationship in Antarctica: Climate Dynamics, v. 36, p. 277-287.

Medley, B., Joughin, I., Das, S.B., Steig, E.J., Conway, H., Gogineni, S., Criscitiello, A.S., Mcconnell, J.R., Smith, B.E., Broeke, M.R., Lenaerts, J.T.M., Bromwich, D.H., and Nicolas, J.P., 2013, Airborne-radar and ice-core observations of annual snow accumulation over Thwaites Glacier, West Antarctica confirm the spatiotemporal variability of global and regional atmospheric models: Geophysical Research Letters, v. 40, p. 3649-3654.

Monaghan, A.J., Bromwich, D.H., Chapman, W., and Comiso, J.C., 2008, Recent variability and trends of Antarctic near-surface temperature: Journal of Geophysical Research: Atmospheres, v. 113.

Monaghan, A.J., Bromwich, D.H., Fogt, R.L., Wang, S., Mayewski, P.A., Dixon, D.A., Ekaykin, A., Frezzotti, M., Goodwin, I., Isaksson, E., Kaspari, S.D., Morgan, V.I., Oerter, H., Van Ommen, T.D., Van Der Veen, C.J., and Wen, J., 2006, Insignificant change in Antarctic snowfall since the International Geophysical Year: Science (New York, N.Y.), v. 313, p. 827.

Naik, S., Thamban, M., Laluraj, C., Redkar, B., and Chaturvedi, A., 2010, A century of climate variability in central Dronning Maud Land, East Antarctica, and its relation to Southern Annular Mode and El Nino-Southern Oscillation: Journal of Geophysical Research-Atmospheres, v. 115.

Rieneker, M.M., Suarez, M., J., Gelaro, R., Todling, R., Bacmeister, J., Liu, E., Bosilovich, M.G., Schubert, S.D., Takacs, L., Kim, G., Bloom, S., Chen, J., Collings, D., Conaty, A., da Silva, A., Gu, W., Joiner, J., Koster, R.D., Lucchesi, R., Molod, A., Owens, T., Pawson, S., Pegion, P., Redder, C., R., Reichle, R., Robertson, F.R., Ruddick, A.G., Sienkiewicz, M., and Woollen, J., 2011, MERRA: NASA's Modern-Era Retrospective Analysis for Research and Applications: Journal of Climate, v. 24, p. 3624-3648.

Steig, E., Schneider, D., Rutherford, S., Mann, M., Comiso, J., and Shindell, D., 2009, Warming of the Antarctic ice-sheet surface since the 1957 International Geophysical Year: Nature, v. 457, p. 459.

Thomas, E.R., Dennis, P.F., Bracegirdle, T.J., and Franzke, C., 2009, Ice core evidence for significant 100-year regional warming on the Antarctic Peninsula: Geophysical Research Letters, v. 36.

Thomas, E.R., Marshall, G.J., and Mcconnell, J.R., 2008, A doubling in snow accumulation in the western Antarctic Peninsula since 1850: Geophysical Research Letters, v. 35.

Thomas, R., Rignot, E., Casassa, G., Kanagaratnam, P., Acuna, C., Akins, T., Brecher, H., Frederick, E., Gogineni, P., Krabill, W., Manizade, S., Ramamoorthy, H., Rivera, A., Russell, R., Sonntag, J., Swift, R., Yungel, J., and Zwally, J., 2004, Accelerated sea-level rise from West Antarctica: Science, v. 306, p. 255-258.

Thompson, D.W.J., and Wallace, J.M., 2000, Annular Modes in the Extratropical Circulation. Part I: Month-to-Month Variability: Journal of Climate, v. 13, p. 1000-1016.

Trauth, M.H., 2007, MATLAB recipes for earth sciences.

Turner, J., 2004, The El Nino-southern oscillation and Antarctica: International Journal of Climatology, v. 24, p. 1-31.

Uppala, S.M., Kallberg, P.W., Simmons, A.J., Andrae, U., Bechtold, V.D.C., Fiorino, M., Gibson, J.K., Haseler, J., Hernandez, A., Kelly, G.A., Li, X., Onogi, K., Saarinen, S., Sokka, N., Allan, R.P., Andersson, E., Arpe, K., Balmaseda, M.A., Beljaars, A.C.M., Van de berg, L., Bidlot, J., Bormann, N., Caires, S., Chevallier, F., Dethof, A., Dragosavac, M., Fisher, M., Fuentes, M., Hagemann, S., Holm, E., Hoskins, B.J., Isaksen, L., Janssen, P.A.E.M., Jenne, R., McNally, A.P., Mahfouf, J.-., Morcrette, J.-., Rayner, N.A., Saunders, R.W., Simon, P., Sterl, A., T renberth, K.E., A.Untch, V., D., Viterbo, P., and Woollen, J., 2005, The ERA-40 re-analysis: Quarterly Journal of the Royal Meteorological Society, v. 131, p. 2961-3012.

Van De Berg W.J, Van Den Broeke M.R.,Reijmer C.H., Van Meijgaard E., 2005, Characteristics of the Antarctic surface mass balance, 1958–2002, using a regional atmospheric climate model: Annals of Glaciology, v. 41, p. 97-104.

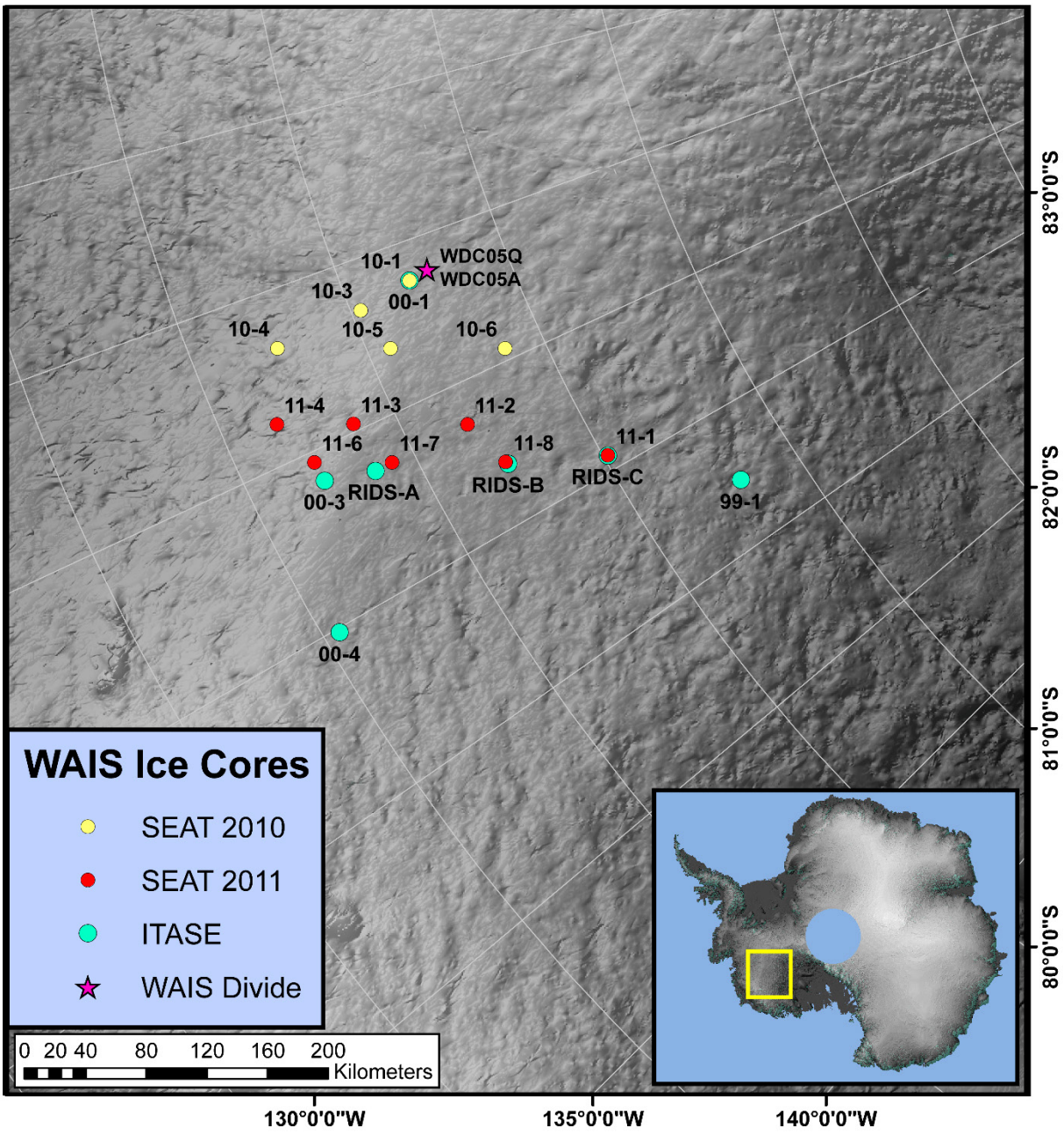

Figure 1: Map of the central WAIS showing locations of SEAT cores and ITASE cores that were drilled in the same region. The WAIS divide deep core is shown for reference.

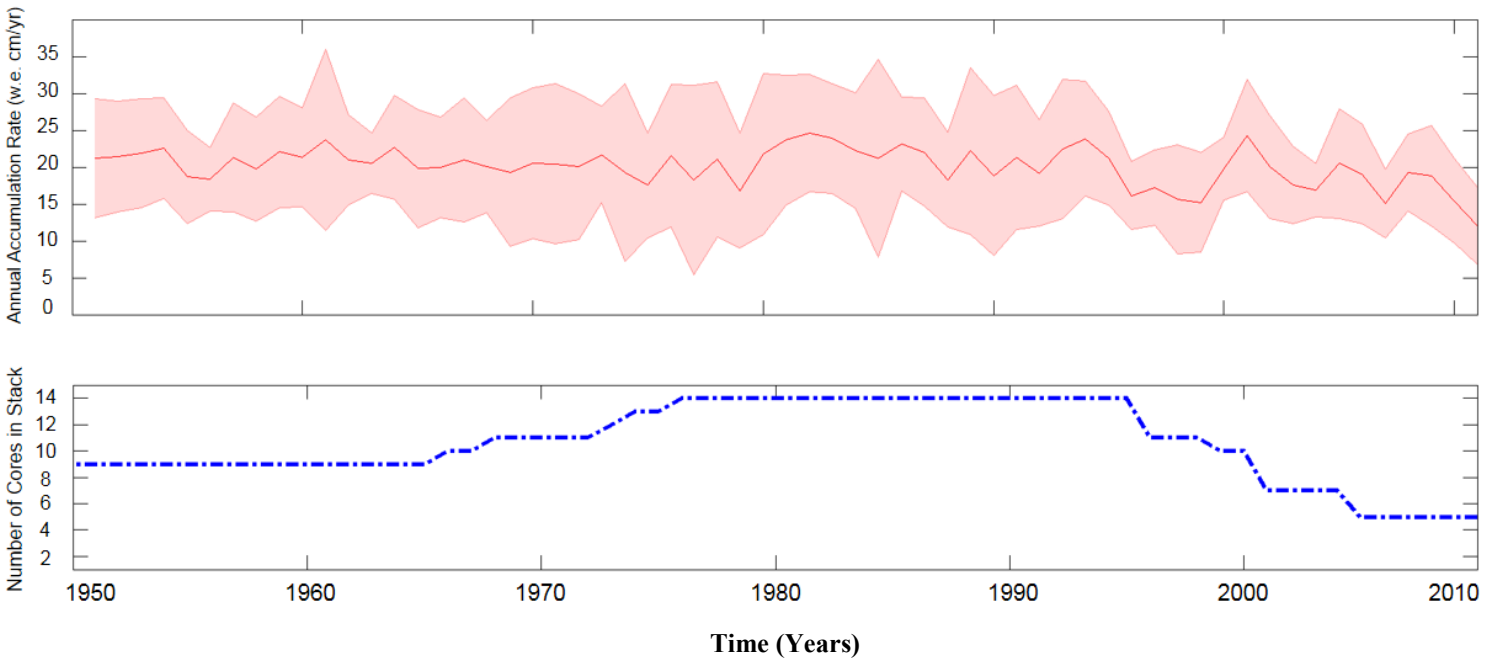

Figure 2: a) Time series of the 14 core stacked record consisting of 5 SEAT and 9 ITASE cores. Red shaded error bars indicate standard error of the stacked record. b) Number of cores in the stacked record over time.

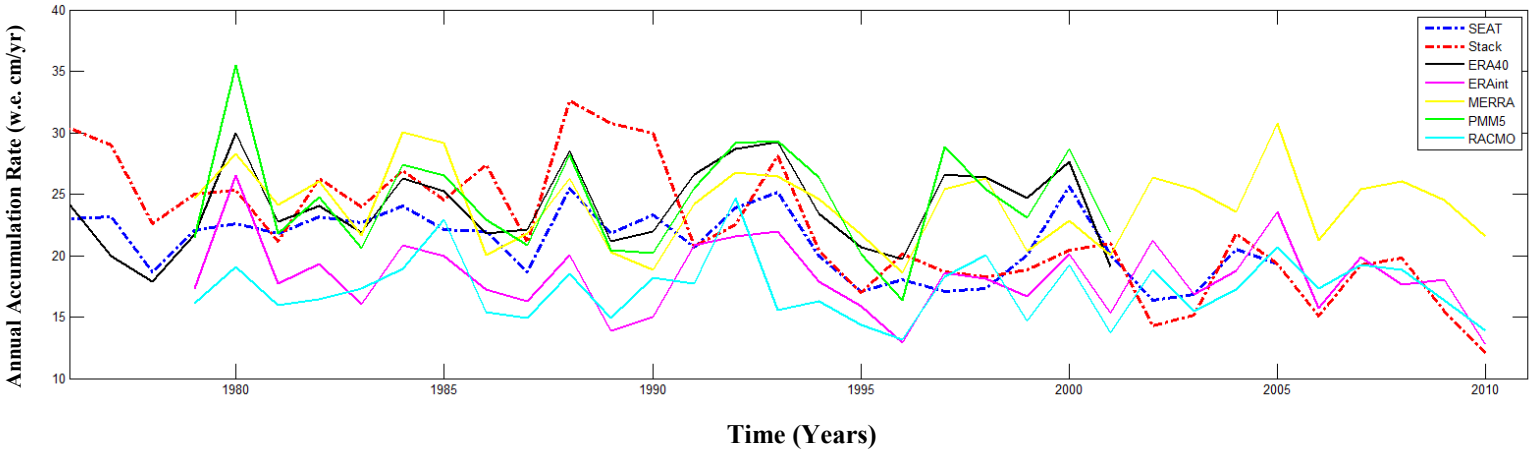

Figure 3: Time series with SEAT 2010 stack, 14 core stack, and five simulated records from different models/reanalyses.

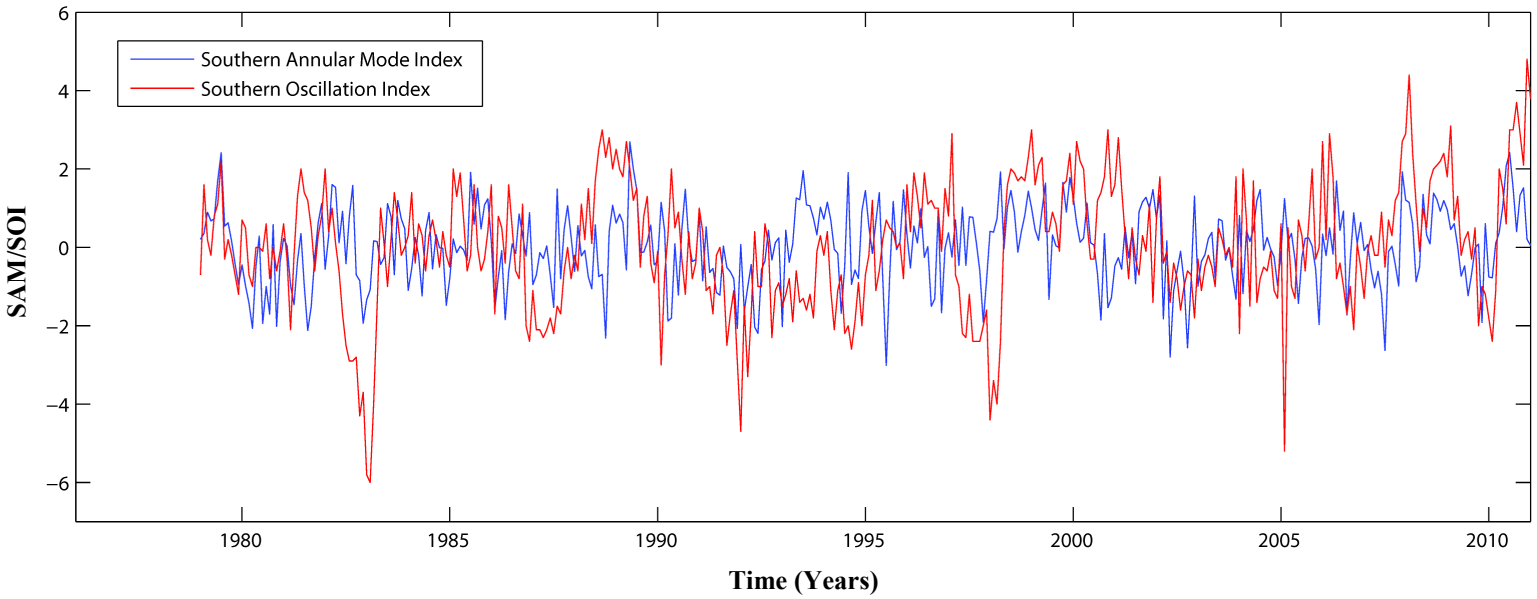

Figure 4: Time series of the Southern Oscillation Index and the Southern Annular Mode Index. These indices are indicators of the phase of SAM and ENSO in a given year.

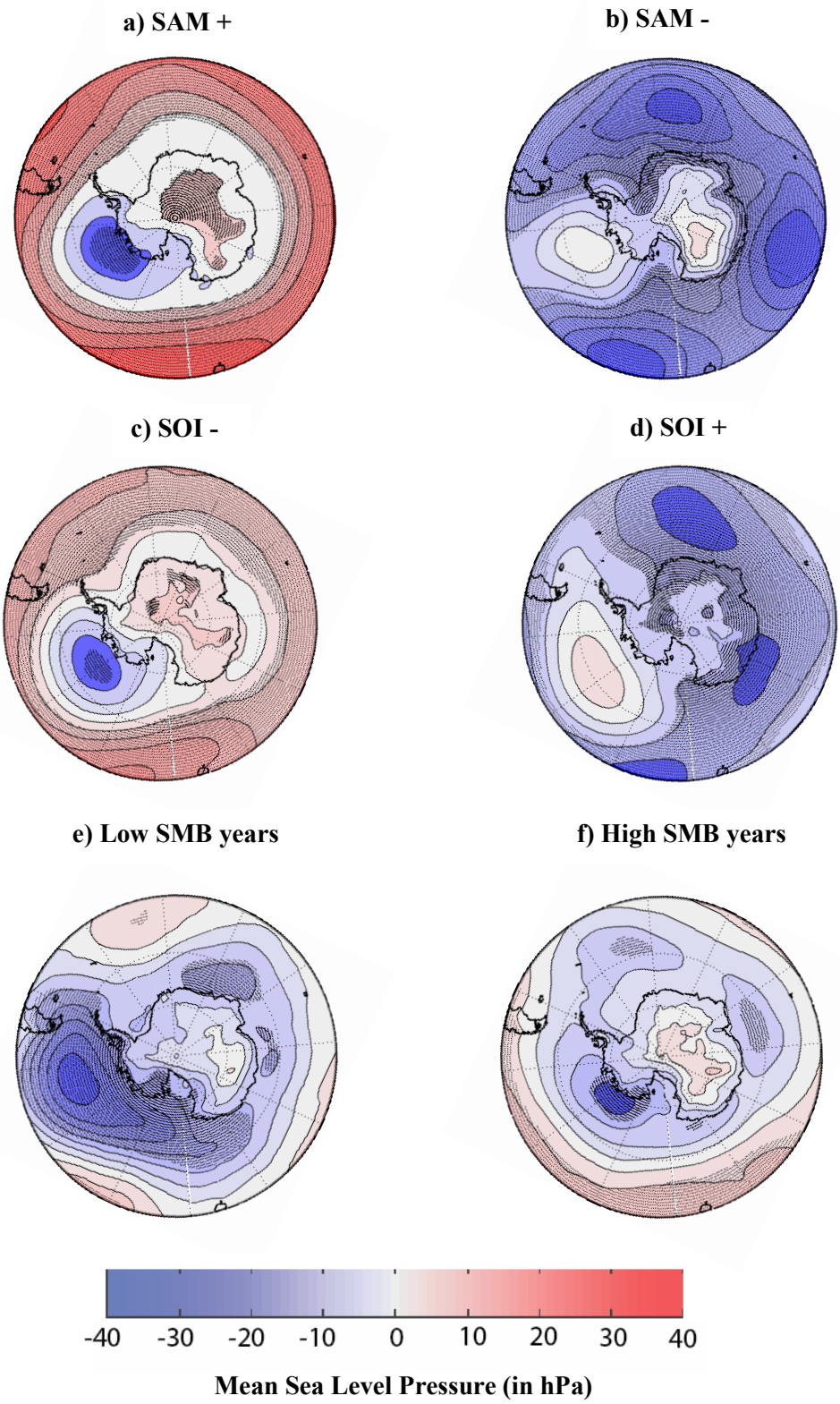

Figure 5: Annual plots of mslp anomalies (in hPa) for a) SAM+, b) SAM-, c) extreme negative years of ENSO, d) positive years of ENSO, e) Years of anomalously low SMB in stacked record, and f) Years of anomalously high SMB in stacked record. Areas shaded with black dots indicate significance at 95% confidence level. Data from ERA-interim

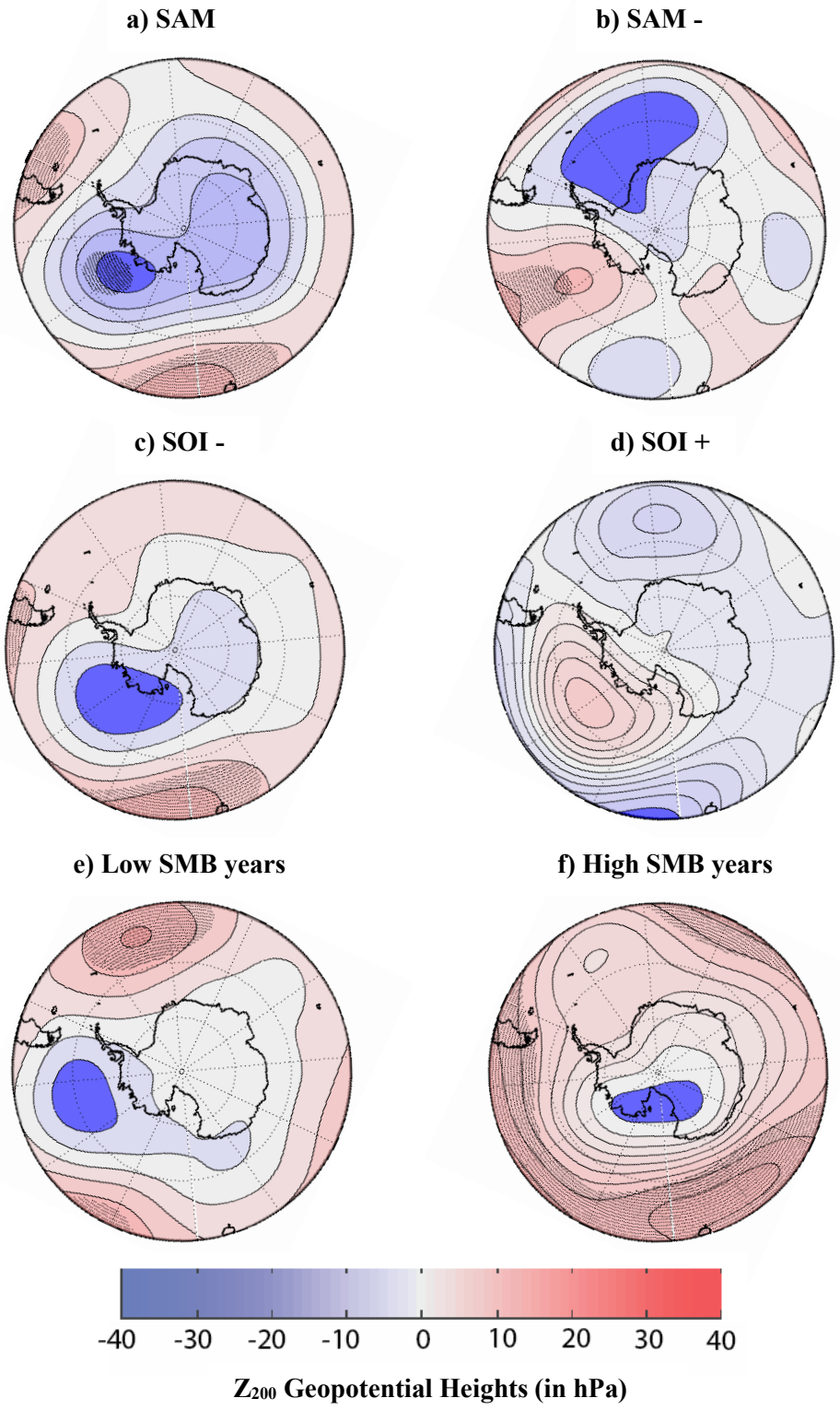

Figure 6: Annual plots Z200 hPa geopotential height anomalies (in hPa) for a) Years of anomalously high SMB in stacked record, b) Years of anomalously low SMB in stacked record, c) extreme positive years of ENSO, d) extreme negative years of SAM, e) extreme positive years of SAM, and f) extreme negative years of ENSO. Areas shaded with black dots indicate significance at 95% confidence level. Data from ERA-interim

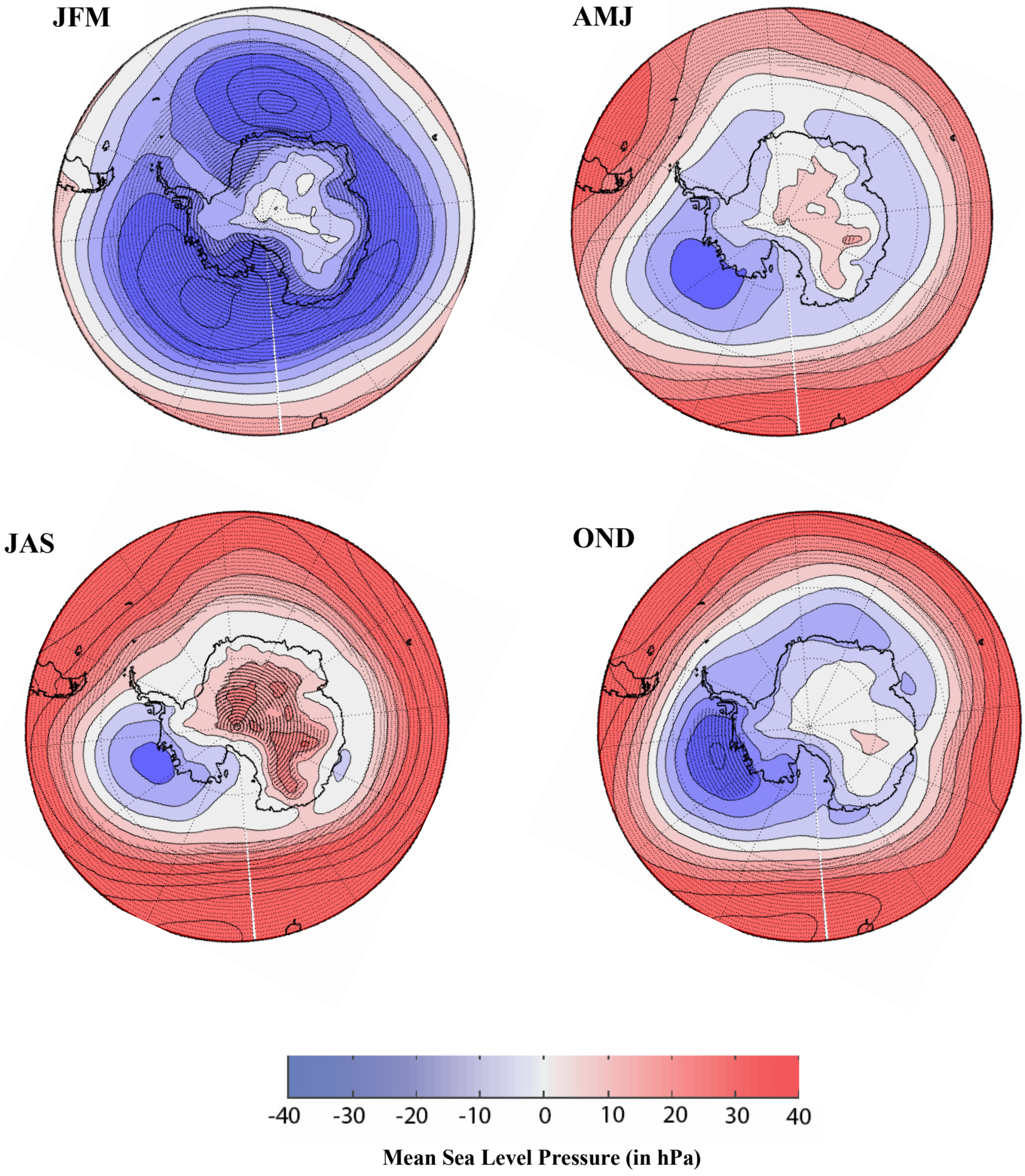

Figure 7: Mean sea level pressure (mslp) seasonal anomalies for the years where the extreme positive phase of SAM occurred over the 33 year period 1979-2011. Areas shaded with black dots indicate significance at 95% confidence level. Data from ERA-interim

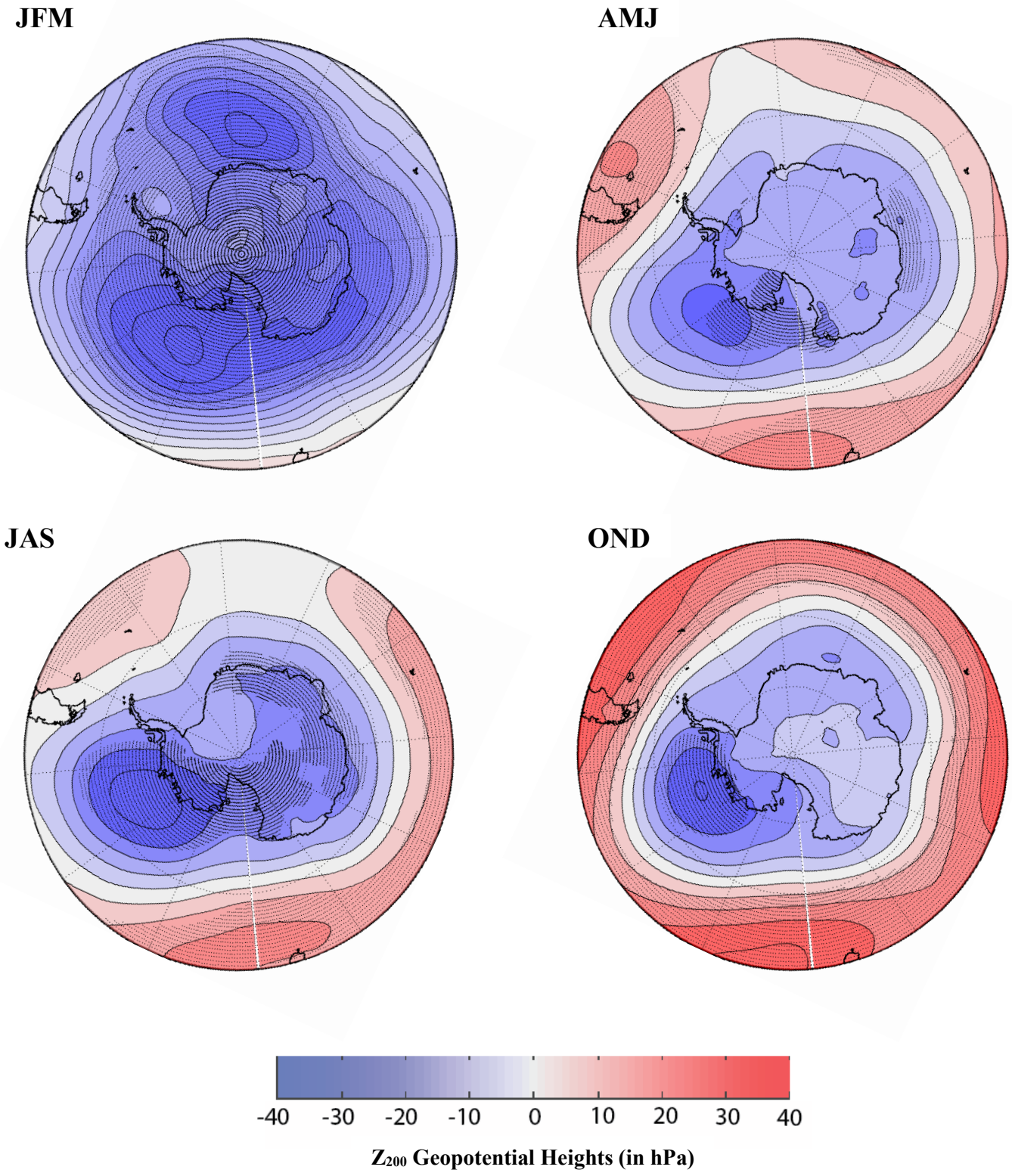

Figure 8: Z_{200} seasonal anomalies for the years where the extreme positive phase of SAM occurred over the 33 year period 1979-2011. Areas shaded with black dots indicate significance at 95% confidence level. Data from ERA-interim

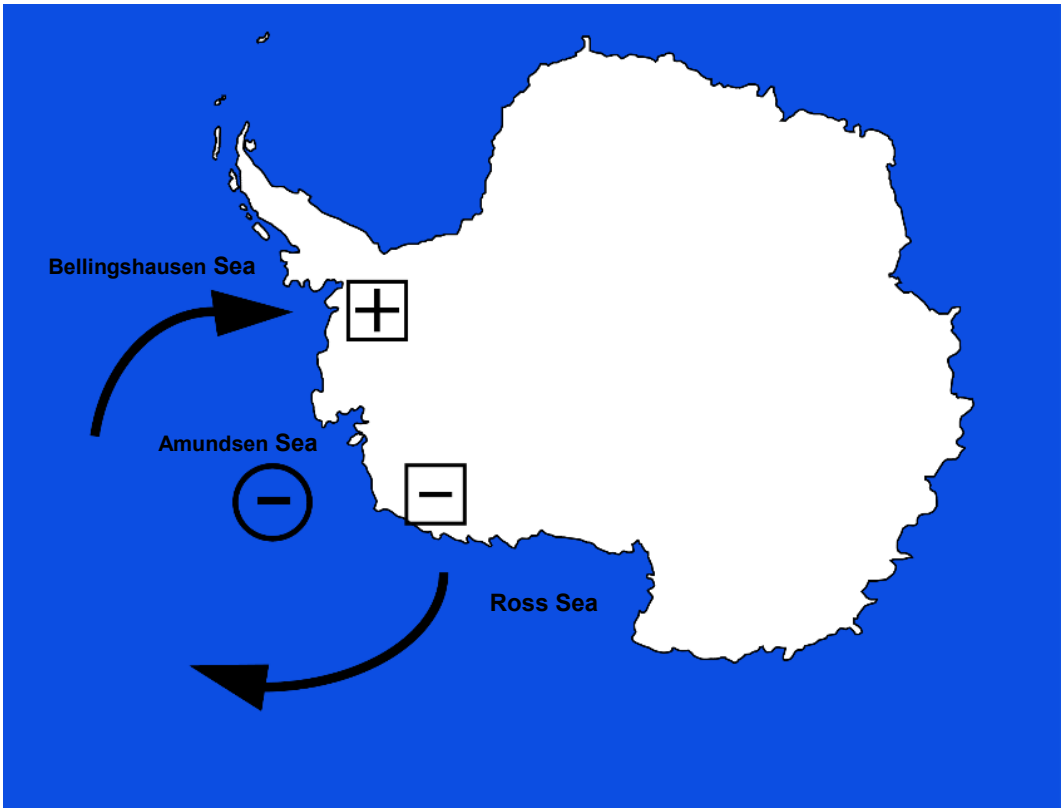

Figure 9: Modified conceptual image from Genthon et al. (2005) showing the effect a low pressure center (minus sign in circle) over the Amundsen Sea has on accumulation rates over WAIS. The low pressure center is associated with the positive phase of the SAM or Negative phase of ENSO. This low results in lower accumulation rates over western WAIS (minus sign in square) and higher accumulation rates near the Antarctic Peninsula (plus sign in square). A greater occurrence of the positive phase of SAM leads to this persistent pattern with greater frequency.

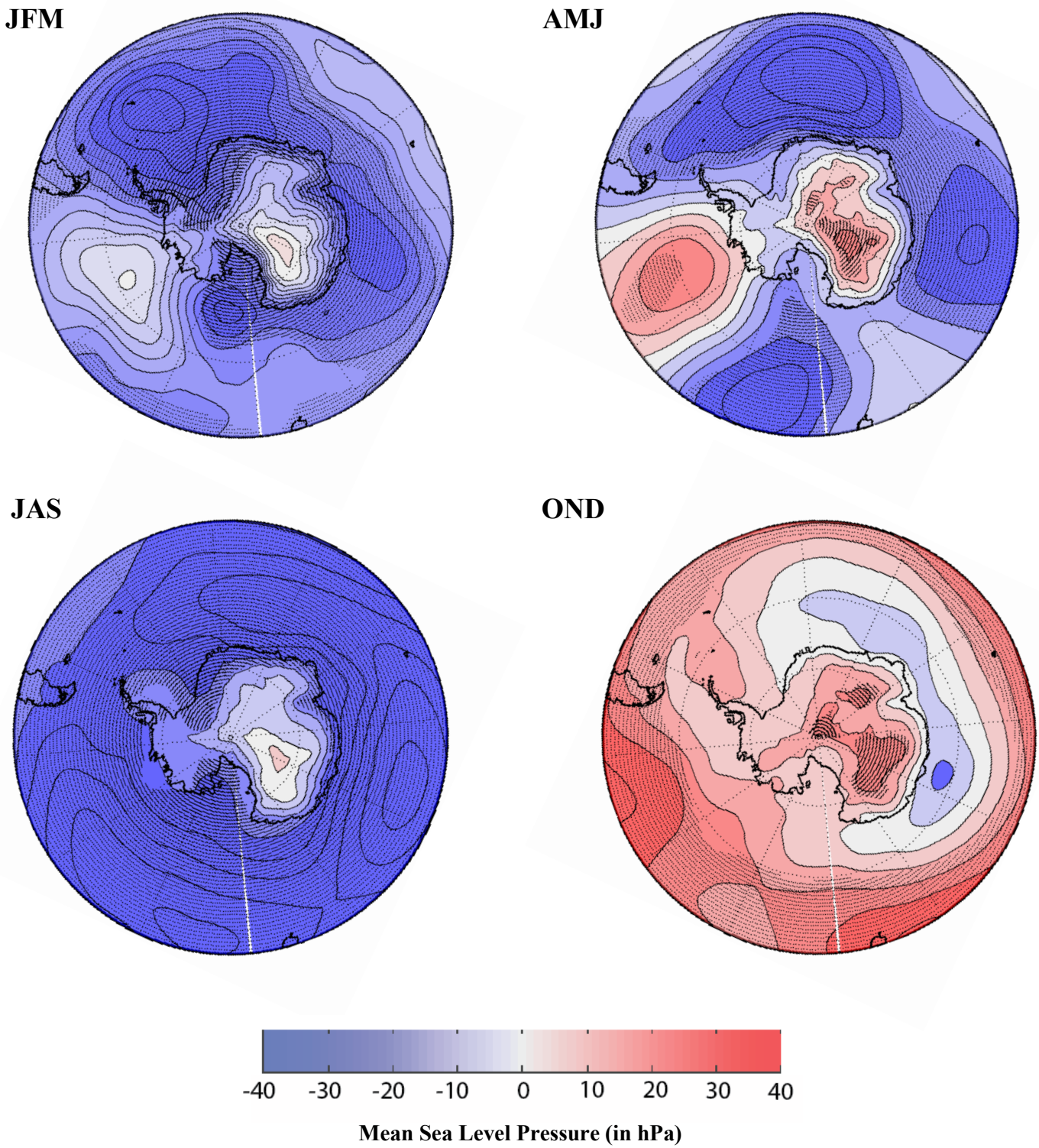

Figure 10: Mean sea level pressure (mslp) seasonal anomalies for the years where the extreme negative phase of SAM occurred over the 33 year period, 1979-2011. Areas shaded with black dots indicate significance at 95% confidence level. Data from ERA-interim

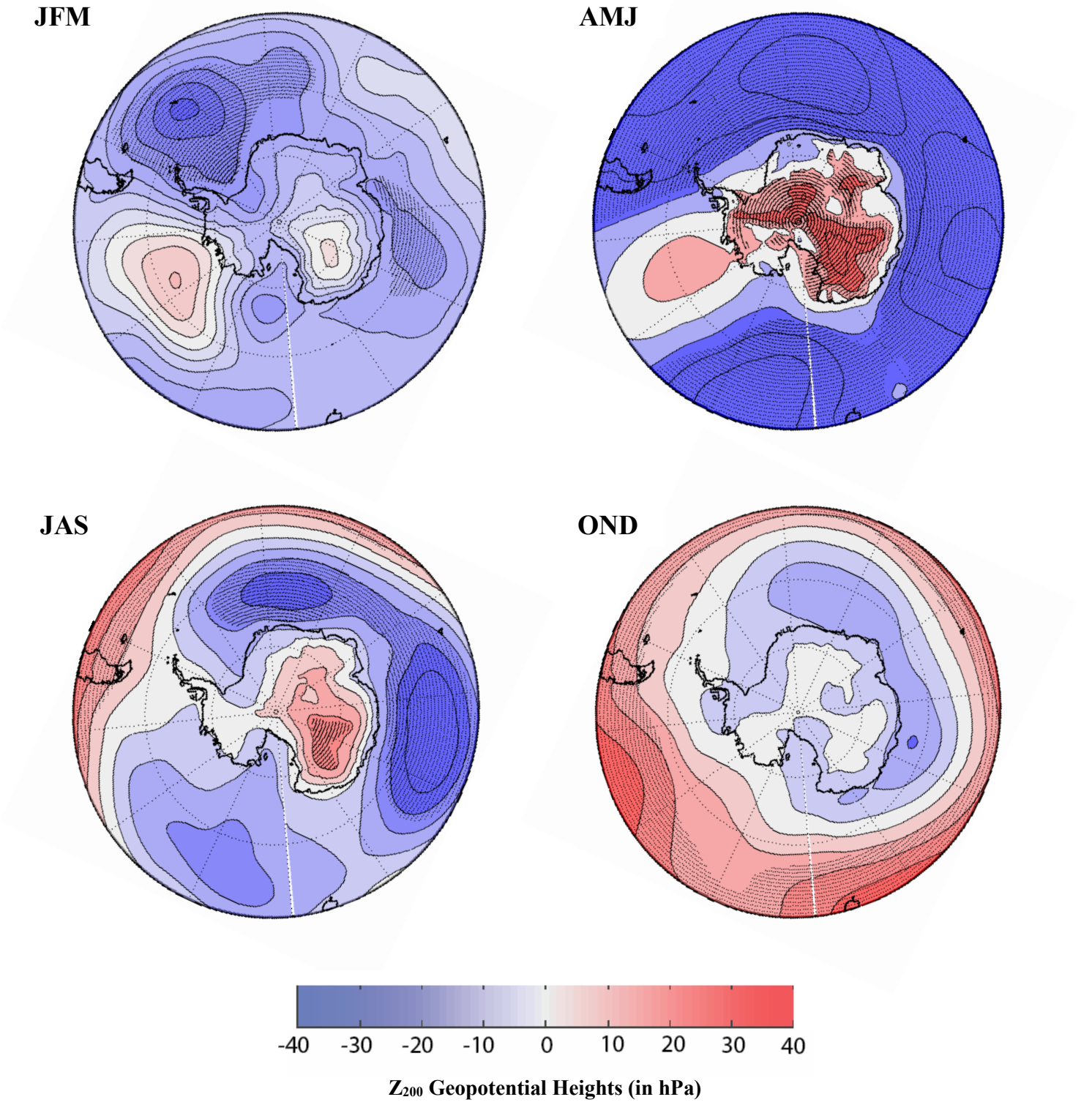

Figure 11: Z_{200} seasonal anomaly plots for the years where the extreme negative phase of SAM occurred over the 33 year period, 1979-2011. Areas shaded with black dots indicate significance at 95% confidence level. Data from ERA-interim

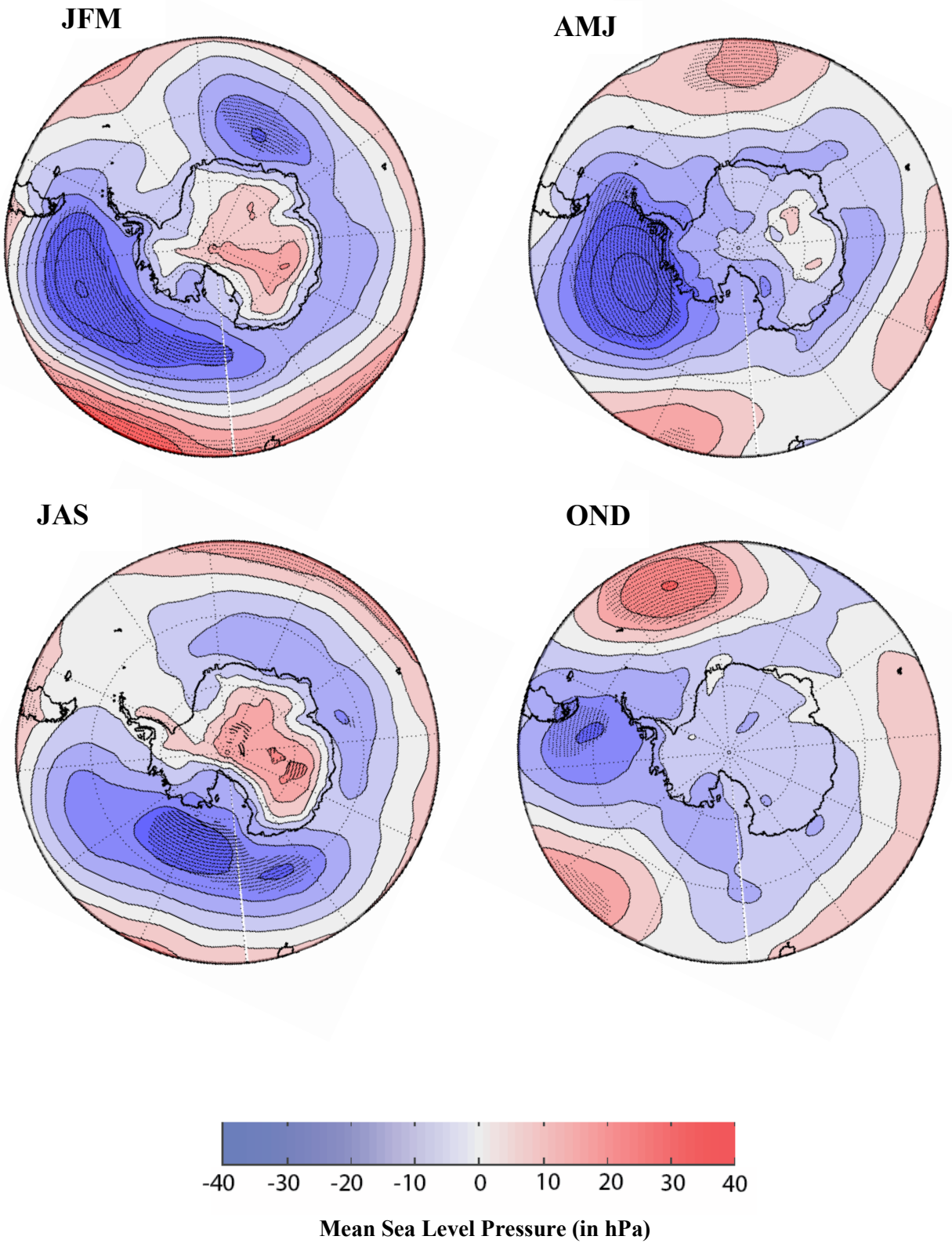

Figure 12: Mean sea level pressure (mslp) seasonal anomalies for the years where SMB in the stacked record was anomalously low over the 33 year period, 1979-2011. Areas shaded with black dots indicate significance at 95% confidence level. Data from ERA-interim

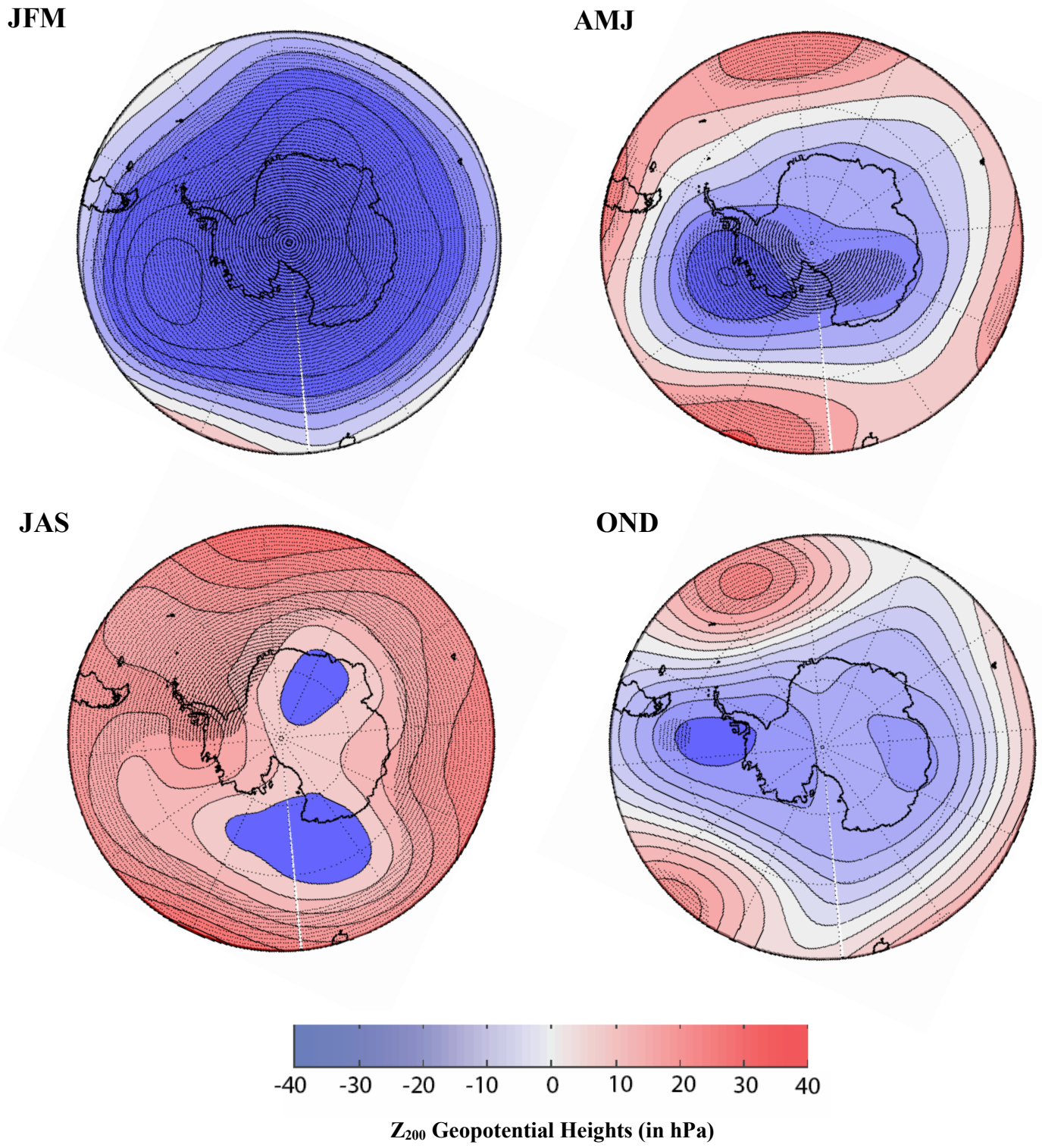

Figure 13: Z_{200} seasonal anomalies for the years where SMB in the stacked record was anomalously low over the 33 year period, 1979-2011. Areas shaded with black dots indicate significance at 95% confidence level. Data from ERA-interim

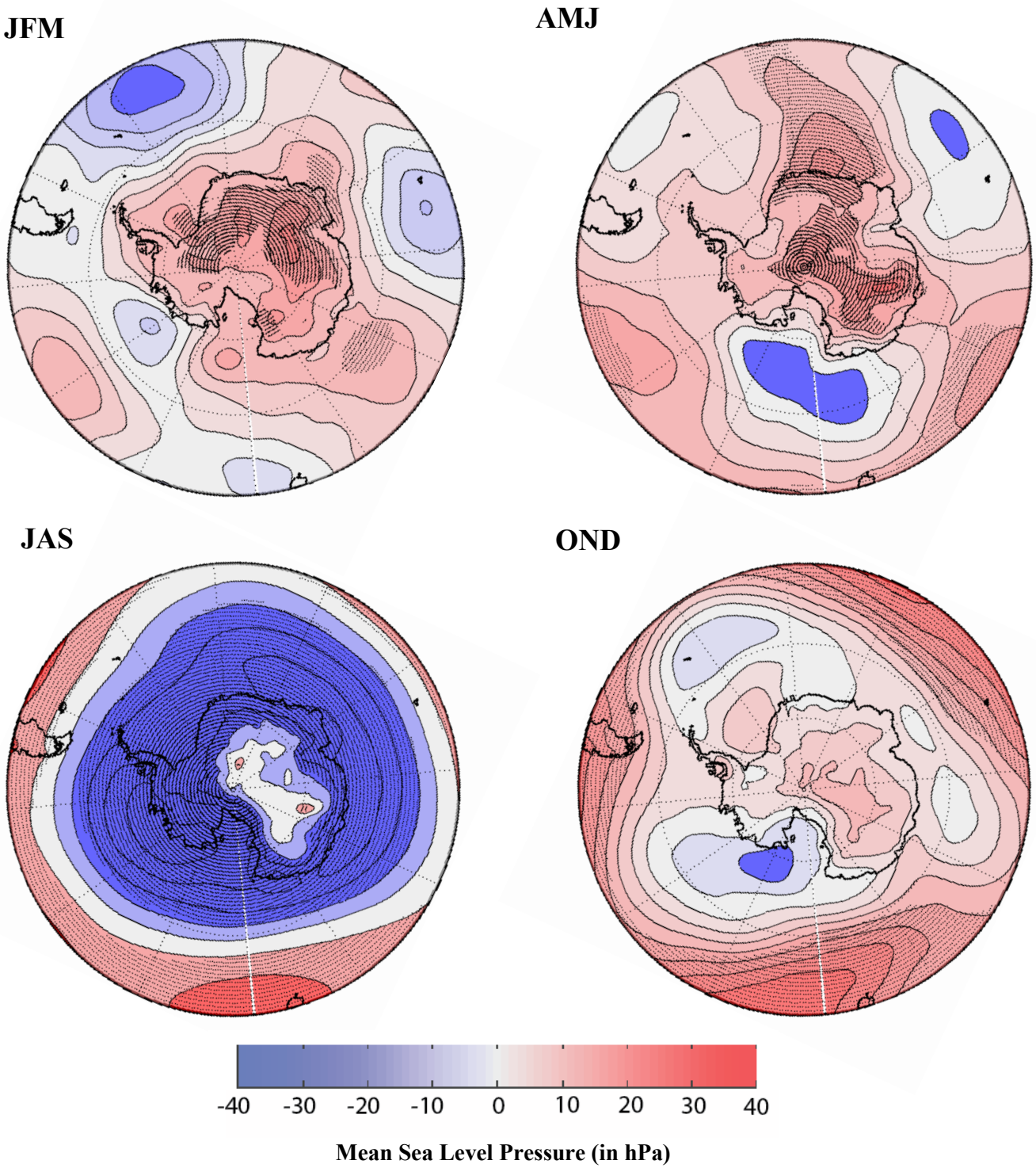

Figure 14: Mean Sea Level Pressure (mslp) seasonal anomalies for the years where SMB in the stacked record was anomalously high over the 33 year period, 1979-2011. Areas shaded with black dots indicate significance at 95% confidence level. Data from ERA-interim

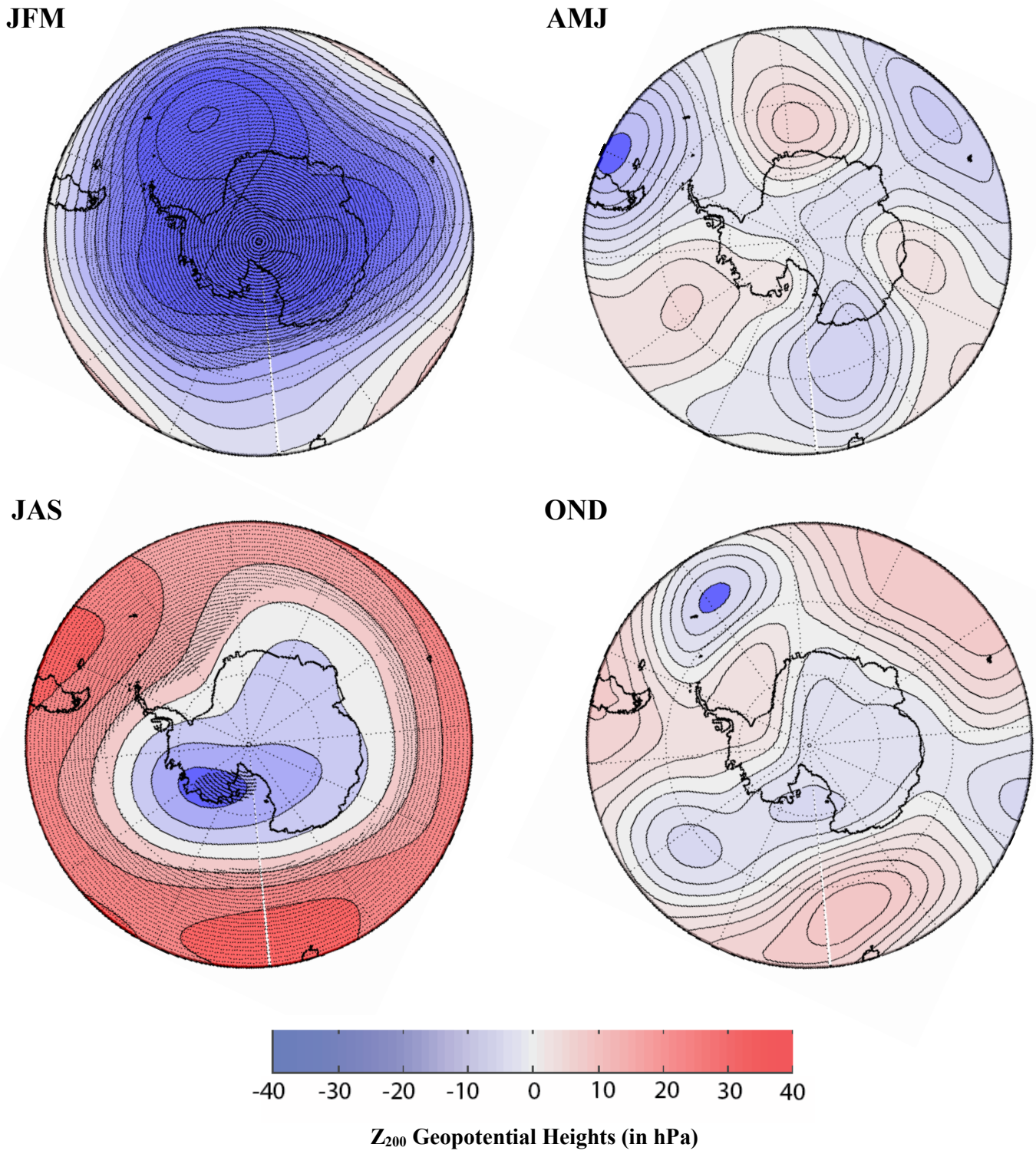

Figure 15: Z_{200} seasonal anomalies for the years where SMB in the stacked record was anomalously high over the 33 year period, 1979-2011. Areas shaded with black dots indicate significance at the 95% confidence level. Data from the ERA-interim

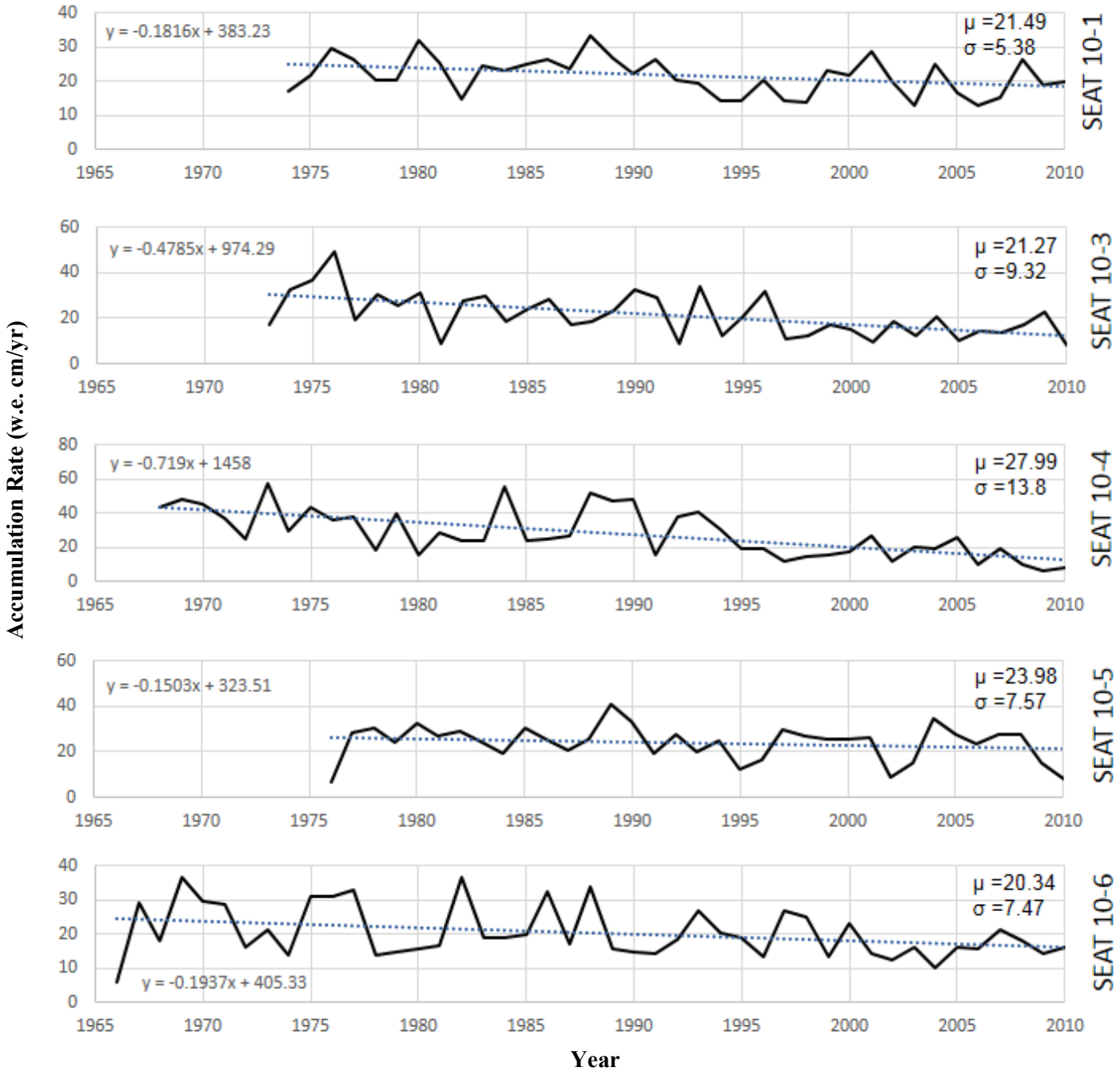

Figure 16: Reconstructed annual SMB for the SEAT 2010 firn cores. All cores have a negative slope indicating a region wide decline in SMB over the past three decades.

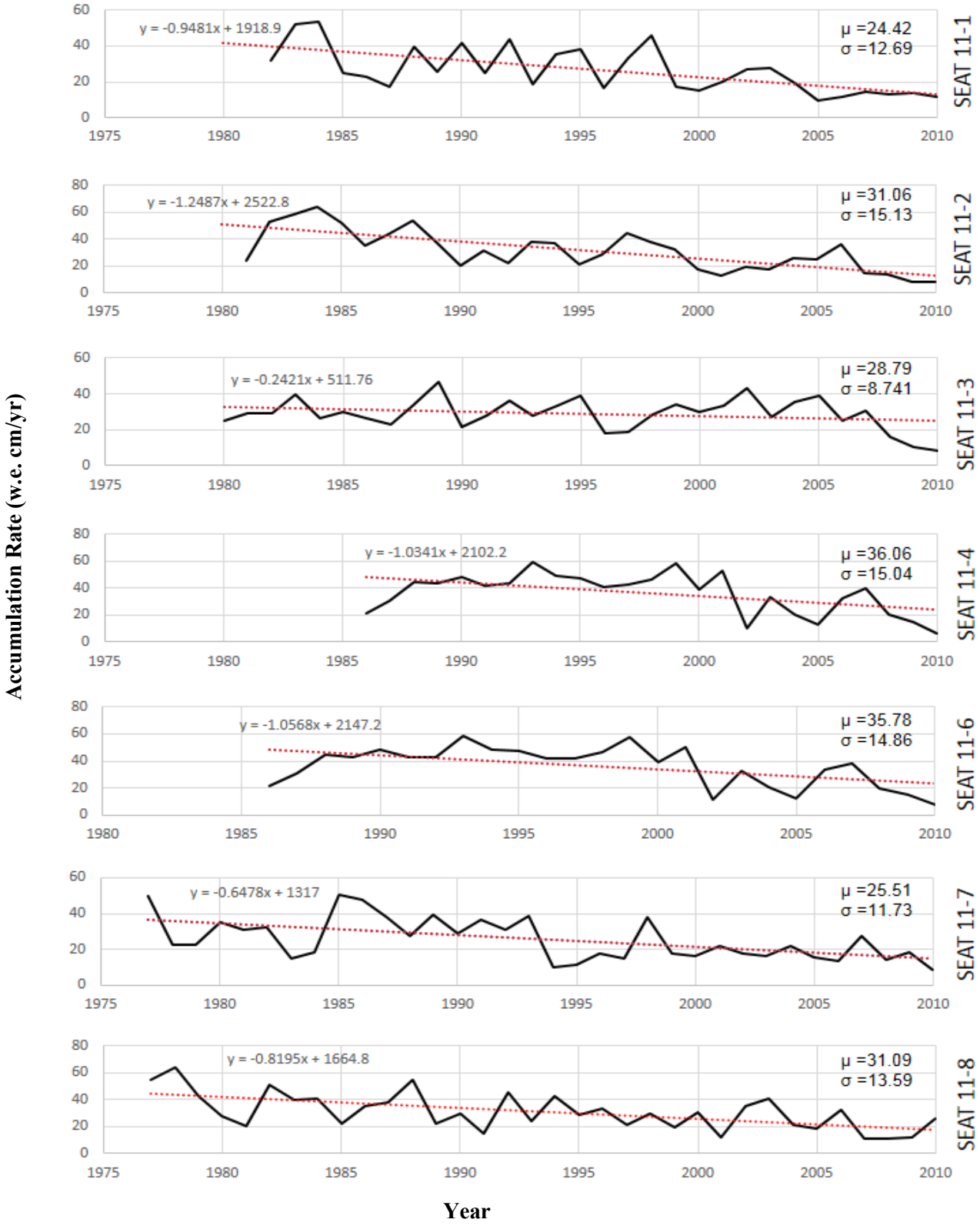

Figure 17: Preliminary reconstructed annual SMB for the SEAT 2011 firn cores. All cores have a negative slope further supporting a region wide decline in SMB over the past three decades.

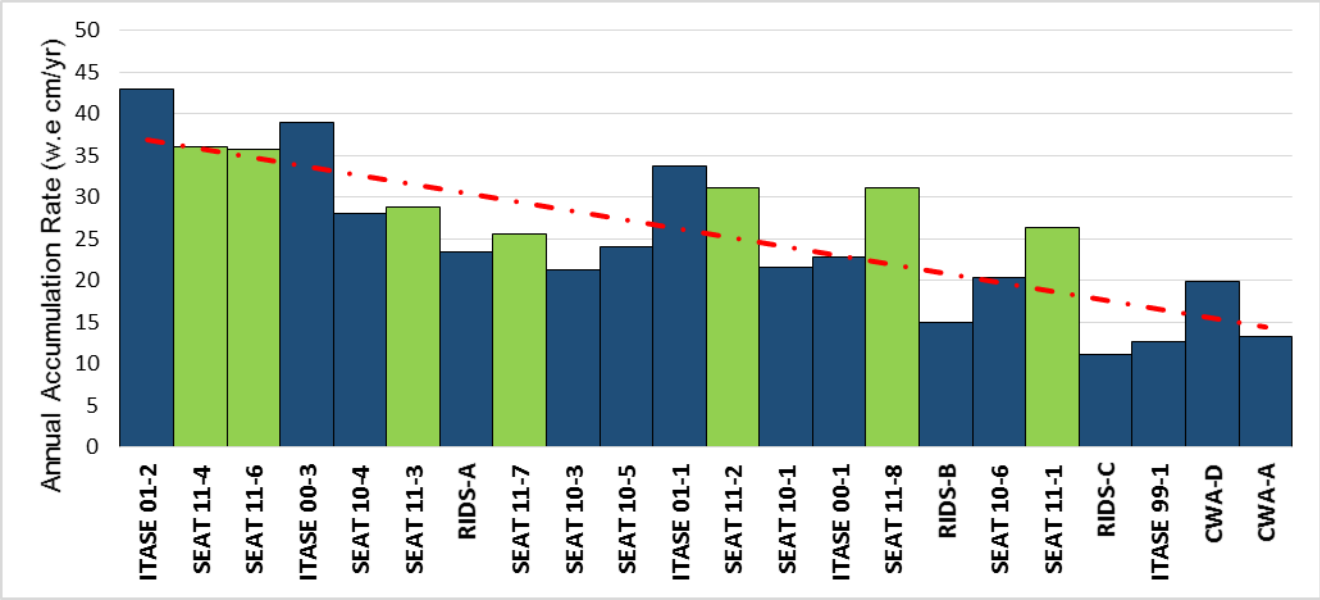

Figure 18: Mean annual SMB (w.e. cm/yr) for 19 firn cores used in this study. The cores are arranged by increasing distance from the coast (from left to right). The preliminary SEAT 2011 cores (green bars) follow the general trend of decreasing accumulation rates as distance from the coast increases.

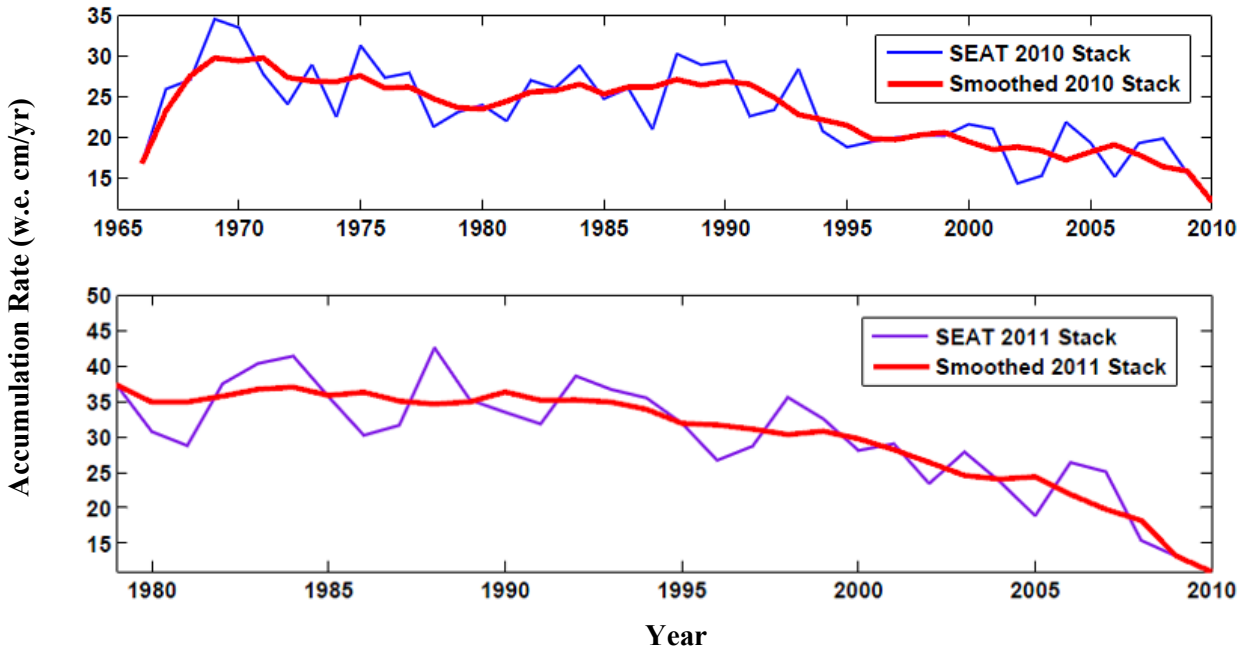

Figure 19: Stacked record for the SEAT 2010 and SEAT 2011 firn cores. Stacked records were smoothed using a five year moving average.